REPORT SERIES IN AEROSOL SCIENCE
N:o 195 (2017)

Modelling studies on the effect of aerosols and cloud microphysics on cloud and fog properties

ZUBAIR MAALICK

Department of Applied Physics
Faculty of Science and Forestry
University of Eastern Finland
Kuopio, Finland

Academic dissertation

To be presented, with the permission of the Faculty of Science and Forestry of the University of Eastern Finland, for public examination in auditorium MS302, Medistudia building, on February 14th, 2017, at noon.

Kuopio 2017

Author's Address: Department of Applied Physics
University of Eastern Finland
P.O.Box 1627
FI-70211 Kuopio, Finland

Supervisors: Research Manager Sami Romakkaniemi, Ph.D.
Atmospheric Research Centre of Eastern Finland
Finnish Meteorological Institute, Kuopio

Researcher Thomas Kühn, Ph.D.
Department of Applied Physics
University of Eastern Finland, Kuopio

Prof. Hannele Korhonen, Ph.D.
Climate Research Unit
Finnish Meteorological Institute, Helsinki

Prof. Ari Laaksonen, Ph.D.
Department of Applied Physics
University of Eastern Finland, Kuopio

Reviewers: Reader Paul J. Connolly, Ph.D.
School of Earth, Atmosphere and Environmental Sciences
University of Manchester, UK

Researcher Risto Makkonen, Ph.D.
Department of Physics
University of Helsinki, Finland

Opponent: Prof. Veli-Matti Kerminen, Ph.D.
Department of Physics
University of Helsinki, Finland

ISBN 978-952-7091-73-9 (printed version)
ISSN 0784 - 3496
Helsinki 2017
Unigrafia Oy

ISBN 978-952-7091-74-6 (pdf version)
http://ethesis.helsinki.fi
Helsinki 2017
Helsingin yliopiston verkkojulkaisut

Acknowledgements

The research activity presented in this thesis was carried out at the department of Applied Physics, University of Eastern Finland.

First and foremost, I would like to express my heartfelt gratitude to my principal supervisor Dr. Sami Romakkaniemi for his continuous support, guidance and encouragement over the last few years. Sami was the person who introduced me to an interesting research topic and provided me with the freedom to explore different directions in the field of aerosols, right from the very beginning. I have learned a great deal from his expertise on the topic and sharp insights from different perspectives. He was always excited about any kind of results, and taught me not only how to interpret the results, but also how to think critically about the problem.

My sincere gratitude is also reserved for my supervisor Dr. Thomas Kuhn for his guidance, assistance, and expertise in helping me to improve my technical skills. I would also like to take this opportunity to thank my other supervisors, Prof. Hannele Korhonen and Prof. Ari Laaksonen, for their support and constructive and valuable comments throughout my doctoral career.

I would like to extend my gratitude to Dr. Harri Kokkola at the Finnish Meteorological Institute (FMI) for his generous support throughout the years. I would also like to thank my all colleagues, especially the modelling team, for all of the "modellers' meeting" discussions that really broadened my view and made me think about my work in different dimensions.

I would like to acknowledge the head of department Prof. Kari Lehtinen, and head of the aerosols group Prof. Annele Virtanen, for financial support during my doctoral studies. They assisted me with funding and providing me with the work facility in order to complete my dissertation.

Furthermore, I would like to extend my thanks to Dr. Risto Makkonen and Dr. Paul J. Connolly for reviewing this thesis, and their valuable comments. I would also like to acknowledge all the co-authors of the papers included in this thesis.

During my doctoral studies, I have had the pleasure of being surrounded by cheerful friends in Kuopio, who provided me with valuable company and made my stay in Kuopio "feel like home". I am deeply grateful to my loving parents and brothers who motivated me to travel far from my home to pursue my dreams. My mother deserves the deepest and warmest thanks I can possibly give. I also want to give my wholehearted thanks to my wife for her support and caring companionship, and a lot of love to my daughter, Hooriya, the source of the calmness in my eyes. I am greatly indebted to my family for their everlasting love, understanding, and patience. Finally, all credit and thanks to God, who bestowed me with the strength and motivation during my journey to finish my doctoral studies, and who provides me with whatever I need in life.

Modelling studies on the effect of aerosols and cloud microphysics on cloud and fog properties

Zubair Maalick

University of Eastern Finland, 2017

Abstract

Atmospheric aerosol particles influence the Earth's climate either directly by scattering and absorbing incoming solar radiation, or indirectly by influencing cloud properties. According to our current understanding, anthropogenic aerosols induce a cooling effect on the Earth's climate, but estimates of the effect's magnitude are very uncertain. To reduce this uncertainty, it is important to gain more knowledge on how aerosols affect cloud properties, and how cloud processing feeds back into aerosol properties.

In this thesis, the high-resolution large eddy model UCLALES is used as main tool to simulate atmospheric dynamics. Aerosol processes are represented in UCLALES using the sectional aerosol module SALSA. The aerosol module SALSA was further developed to cover cloud droplets and precipitation with a sectional representation. With this tool, it is possible to study the aerosol effect on cloud and fog properties in different atmospheric conditions in more detail than before.

In this thesis, the developed model is employed to address different research questions. It has been suggested that marine cloud brightening (MCB) is an efficient and cost effective geoengineering solution to counteract climate warming. Here, it is shown that the efficacy of the method has previously been overestimated. By accounting for all of the different microphysical processes affecting aerosol particles, the aerosol dispersion in the boundary layer was found to be less efficient than expected, and thus, the proposed emission fluxes need to be re-estimated. The effect of aerosols on radiation fogs was also simulated, and it was found that aerosols, as cloud condensation nuclei (CCN), have a significant effect on the radiation fog life cycle. This effect was significantly enhanced by positive feedback mechanisms. Beyond radiation fog, the skill of UCLALES-SALSA in simulating the dynamics of marine stratocumulus clouds and their dependence on aerosols was demonstrated. As a last topic, another large eddy model, PALM, was employed together with a cloud parcel model to simulate how the surface topography affects cloud droplet formation in low altitude clouds. These simulations were performed for the measurement station at Puijo tower, which lies on top of Puijo hill. Simulations show that the high orographic updrafts on the slopes of the hill can cause the in-cloud formation of droplets, leading to a bi-modal cloud droplet distribution.

The results in this thesis demonstrate the importance of using detailed aerosol representation in cloud-resolving models when aiming to understand cloud-aerosol interactions. It is shown that, in order to reduce the uncertainties associated with aerosol-cloud interactions, not only a detailed understanding of how aerosol affects clouds is required, but an understanding of the associated feedback mechanisms is essential as well.

Keywords: aerosol-cloud interaction, large eddy model, microphysics, radiation fog.

Contents

List of publications

This thesis consists of an introductory review followed by four research articles. In the introductory part, the papers are cited according to their roman numerals. The papers are reproduced under the Creative Commons Licence.

I Maalick Z, Korhonen H, Kokkola H, Kühn T, Romakkaniemi S.: Modelling artificial seasalt emissions in large eddy simulations. *Phil. Trans. R. Soc. A.*, 372, 20140051, 2014.

II Maalick Z, Kühn T, Korhonen H, Kokkola H, Laaksonen A, Romakkaniemi S.: Effect of aerosol concentration and absorbing aerosol on the radiation fog life cycle. *Atmos. Environ.*, 133, 26-33, 2016.

III Tonttila J., Maalick Z., Raatikainen T., Kokkola H., Kühn T., Romakkaniemi S.: Introducing UCLALES-SALSA: a large-eddy model with interactive sectional microphysics for aerosols, clouds and drizzle. *Geosci. Model Dev.*, 10, 169-188, 2017.

IV Romakkaniemi S., Maalick Z., Hellsten A., Ruuskanen A., Ahmad, I., Tonttila, J., Mikkonen S., Komppula M., Kühn T.: Aerosol-landscape-cloud interaction: Signatures of topology effect on cloud droplet formation. under review for *Atmos. Chem. Phys.*

1. Introduction

The atmospheric boundary layer (ABL) is the part of the atmosphere in which the effects of the Earth's surface on the atmosphere are directly felt, on time scales of less than a day (Stull, 1988). Many of the atmospheric phenomena we experience in our daily lives are special characteristics of the ABL, and cannot be experienced in the upper part of the atmosphere. The thickness of the ABL ranges from 10 m to 3000 m depending on the geographical location, season and time of day. An interesting feature of the ABL is the presence of clouds, which not only participate in the hydrological cycle (Seinfeld and Pandis, 2006), but also strongly affect the Earth's radiation budget. They exert a cooling influence on the Earth's atmosphere by reflecting incoming short wave (SW) radiation back into space, but also absorb and re-emit outgoing longwave (LW) radiation, causing warming. The radiative properties of clouds depend mainly on their thickness and location in the atmosphere, but also on their microphysical properties. Another important aspect of the ABL environment is the presence of turbulence, formed of different sized eddies that interact with each other. Eddies form when thermals of warm air rise due to surface heating, cold air sinks due to radiative cooling, or simply due to the interaction between wind and surface (Stull, 1988). The top of the ABL is commonly determined by a sharp increase in temperature (creating a so-called inversion), which separates the mixed layer from the so-called free atmosphere. This layer traps turbulence, pollutants, and moisture below it, and prevents most of the surface friction from being felt by the free atmosphere. Turbulence in the ABL affects the exchange of heat, mass, and momentum at the surface, and thereby plays a major role in modulating the weather (temperature, humidity, wind strength, air quality, etc.).

An aerosol is a mixture of gases and microscopic solid or liquid particles floating in the atmosphere (Hinds, 1999). These particles are present in a multitude of forms and sizes, and originate from various sources. The size of atmospheric aerosol particles ranges from very small molecular clusters of 1-2 nanometres (nm, 10^{-9}m) up to ~10 micrometres (μm**,** 10^{-6}m). The concentration of aerosol particles in the atmosphere also varies between different regions and seasons. In a very clean environment, like the polar regions, aerosols are present in concentrations as low as a few tens of particles per cm^3 (Väänänen et al., 2013; Järvinen et al., 2013)**.** On the other extreme, aerosol concentrations in highly polluted metropolitan/industrial cities can exceed 10^5 particles per cm^3 (Wu et al., 2008; Mönkkönen et al., 2005). Globally, the most abundant aerosol chemical components are sulphates, nitrates, black carbon, organic carbon, sea-salt and mineral dust. Atmospheric aerosols affect human health (Holland et al., 2005), climate (IPCC, 2013) and visibility (Chang et al., 2007).

The atmospheric lifetime of aerosols spans from a few hours to a few weeks (Williams et al., 2002) and during that time, they undergo various microphysical and chemical processes, which continuously change their properties. From the point of view of affecting the climate, it is attributed that aerosols alter the global radiation budget (Haywood et al., 2009; Forster et al., 2007), either directly, through aerosol-radiation interaction (ARI), or indirectly through aerosol-cloud interaction (ACI), where aerosols modify the cloud droplet number

concentration by acting as a cloud condensation nuclei (CCN), a seed for droplet formation (IPCC, 2013). The net contribution of anthropogenic aerosols, including both ARI and ACI, to radiative forcing is negative. However, absorbing aerosols like black carbon heat the atmosphere locally by absorbing shortwave radiation, thus making a positive contribution to radiative forcing (Bond et al., 2013). As the properties of clouds and aerosols are extremely variable both in space and time, it is difficult to estimate the magnitude of the aerosol effect on climate, especially regionally.

The uncertainties in the estimation of aerosol-induced radiative forcing can be reduced by integrating data from different platforms (ground-based networks, satellite, aircraft, etc.) and techniques (in-situ measurement, remote sensing, and numerical modelling) (Penner et al., 1994; Heintzenberg et al, 1996; Diner et al., 2004). According to the current estimates, the greatest uncertainties in understanding the current climate change trends are around the role of ACI. The understanding of ACI has increased in recent years, but it is still inadequate, because of the large range of scales on which the different processes involved take place. In order to increase our understanding of ACI, different measurement and modelling techniques are needed to address these different scales, which makes it more difficult to study the entity of ACI as a whole (Seinfeld et al., 2016). However, the improvement of the observational tools and numerical models is an ongoing process. Representing ACI in numerical models is challenging, because processes acting on small scales have large-scale consequences, such as changes in cloud cover and cloud organisation. Global models, which have low spatial resolutions, are unable to resolve ABL dynamics or clouds at small scales. Increases in model resolution are limited by the availability of computational resources. Explicit numerical simulations of these processes, even at the scale of entire clouds or multi-cloud systems, require hundreds of hours on the most powerful computers available. Therefore, modellers have to resort to simple parametric representations of these processes in large-scale atmospheric models.

One approach to overcome these limitations has been to run a global climate model with a high resolution (e.g. 3.5 km has been used by Tomita et al., 2005) for a short period of time, so that the largest convective clouds could be represented also on the global scale (Putman and Suarez, 2011). However, due to the high computational demand involved, such climate simulations are not feasible. Another approach is "super parameterization", where a cloud-resolving model (CRM) is embedded into each cell of a large-scale model as a compromise between process level and global-level models (Randall and khairoutdinov, 2003; Grabowski and Smolarkiewicz, 1999; Tao et al., 2009). This has been successful in getting reliable results (Pritchard and Somerville, 2010; DeMott et al., 2011). Both of the above-mentioned approaches provide a platform to study cloud-resolved circulation at the global level, but still lack the ability to resolve cloud processes which, sometimes, require resolutions as high as a few metres. Meso- or regional scale models with high resolutions, starting from tens of kilometres, can also resolve ABL clouds. With the help of such high-resolution models, it is possible to study ACI under idealised conditions or with known boundary conditions. Such high-resolution models have been very successful in understanding cloud processes, turbulent mixing, convection, meso-scale circulation and precipitation and aerosol-cloud interactions (e.g. Rosenfeld et al., 2014). In particular, the large eddy simulation (LES) models, with their

ability to simulate turbulence and cloud systems at a high resolution, have proved to be a useful tool in studying the different types of clouds and their sensitivity to different meteorological conditions (Stevens et al., 2005; Ackerman et al., 2009; Stevens and Seifert, 2008; Seifert et al., 2015) and also to aerosols (Jenkins et al. 2013a; Xue and Feingold 2006). Such models cannot provide us with quantitative global estimates of radiative forcing, but can provide realistic insight into the magnitude of the effect of small-scale interactions (IPCC 2013).

In this thesis, the importance of representing aerosols and cloud microphysics in a cloud scale model, to study ACI, is discussed.

The key objectives of this thesis are:

- To develop a high resolution LES model with realistic aerosol representation to study the microphysics of aerosol-cloud interactions, and to employ the model to demonstrate the importance of microphysical processes on cloud dynamics.
- To study the dispersion of sea-salt particles from artificially injected sea spray in order to understand how different aerosol processes affect particle dispersion in a marine environment. This will help us to assess the efficacy of a geoengineering technique called “marine cloud brightening (MCB)”.
- To quantify the role of aerosols in the radiation fog life cycle. It is hypothesised that aerosols are the main reason for the observed decline in fog events in Europe over the last two decades. To test this hypothesis, the sensitivity of radiation fog to changes in aerosol concentration and radiative properties is explored.
- To assess in detail how aerosol particles activate into cloud droplets both in stratus clouds and in radiation fogs.

We implement aerosol microphysics in the LES model UCLALES (The University of California, Los Angeles – Large Eddy Simulation, Stevens et al., 2005), which is specifically designed to study boundary layer processes. To represent aerosols in UCLALES, we used the already existing aerosol module SALSA (Sectional Aerosol module for Large Scale Applications, Kokkola et al., 2008) and during the thesis, we extended SALSA to also cover cloud microphysics. The new UCLALES-SALSA allows us to study ACI and ARI at a cloud resolving scale, with a resolution as high as a few metres. This thesis is organised as follows: Section 2 discusses clouds and fog formation in detail. Further, ACI and ARI are also discussed in this section. Section 3 contains a description of the main aerosol microphysical processes. An overview of the modelling tools used in this thesis can be found in Section 4. Section 5 discusses the application of the models and the results obtained. Conclusions and final remarks are discussed in Section 6. A brief review of papers and author's contribution are both given in Section 7.

2. Aerosol effect on climate

From the climatic point of view, the importance of aerosols is based on their ability to affect atmospheric radiation transfer. Contrary to greenhouse gases (GHG), aerosols induce an overall cooling effect. However, the aerosol effect on climate is still poorly quantified, because the estimations of radiative forcing vary greatly from observations to models, and even between different models. Unlike most GHGs, atmospheric aerosols are short-lived, and thus their concentrations vary a lot both spatially and temporally, with a strong dependence on the distance from the emission sources. Such a large variability in conditions also hinders the observational and modelling studies of the effect of aerosols on climate. This section provides background information on aerosol interaction with radiation, clouds and fogs, which is necessary to understand how aerosols affect atmospheric radiative transfer.

2.1. Aerosol cloud interaction

A cloud forms from a population of small water droplets or ice crystals suspended in the atmosphere. Clouds, which cover around 2/3 of the Earth's surface (on an annual average), play a major role in maintaining the Earth's radiative balance. They take part in the hydrological cycle, the vertical transport of energy and chemical species, the removal of gases and particles from the atmosphere (wet deposition), and act as medium for aqueous phase chemical reactions (Seinfeld and Pandis, 2006). Clouds can be classified into different types depending on the region in which they form, their altitude, and their structure (Jacobson, 2005). The thread-like, hairy cirrus clouds are formed in the upper part of the troposphere (5 - 14 km). Due to the cold temperatures, they are usually formed of ice crystals. Cumulus clouds are dense clouds with visually sharp edges, with a cloud base as low as 500 m, and with a highly variable vertical extent – from less than 1 km up to several kilometres. These towering clouds are called cumulus congestus. They normally form due to surface-induced convection in warm conditions. These clouds can grow to even larger sizes, reaching the tropopause and forming cumulonimbus (thunderstorm) clouds. Beyond cumulus, another important ABL cloud type is the stratocumulus cloud. Stratocumulus clouds usually form quite uniform cloud decks with a high cloud coverage. They are commonly found at very low levels (less than 2000 m), and especially in marine environments. In addition, different uniform stratus clouds can also be found and, depending on their altitude, named altostratus, nimbostratus, or cirrostratus clouds. Fogs and mists also contain cloud droplets, but they are not classified as clouds because of their own characteristics and formation mechanisms close to the surface (Jacobson, 2005).

In the atmosphere, water vapour needs aerosol particles to condense on in order to form cloud droplets. With a constant amount of water vapour and under the same meteorological conditions (temperature and relative humidity), an increase in aerosol loading would result in more, but smaller, cloud droplets. This increase in the cloud droplet number concentration (CDNC) increases the cloud albedo, which causes the cloud to reflect more solar radiation back into space (Fig. 1). This effect is known as the first aerosol indirect effect or "*Twomey effect*" (Twomey, 1977). A decrease in initial cloud droplet size can also delay precipitation formation,

because the droplets need to exceed a certain size in order to initiate precipitation. This delay in precipitation results in an increase in the vertical growth and lifetime of the cloud, and has been termed the second indirect effect or "*Albrecht effect*" (Albrecht, 1989). In addition, aerosols may absorb solar radiation and warm the surrounding air, which leads to the evaporation of cloud droplets (without directly participating in cloud microphysics). This is called the *"semi direct"* effect.

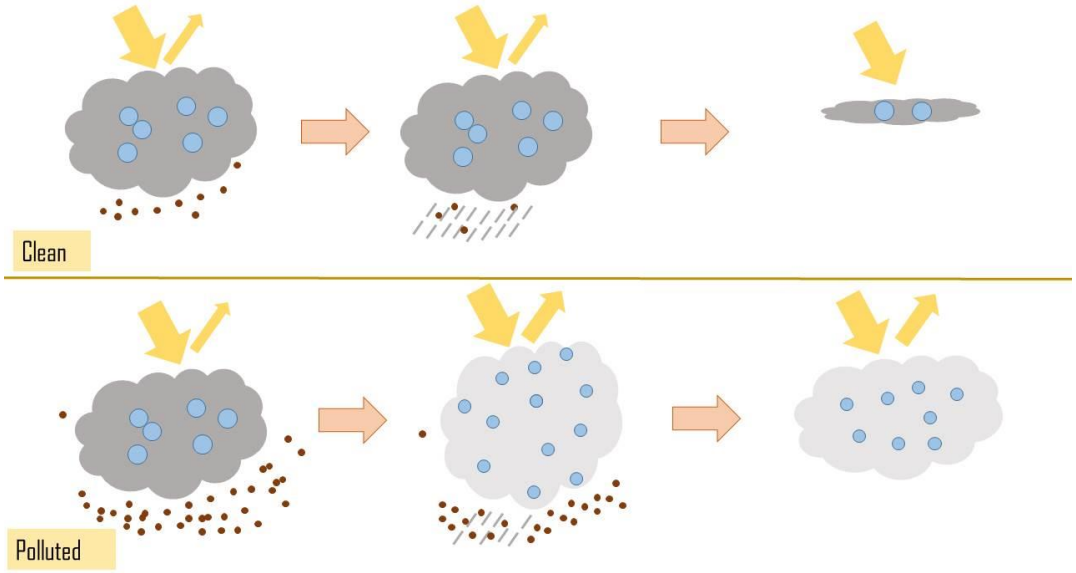

Figure 1: A schematic representation of both the Twomey and Albrecht effects, showing how a polluted cloud is optically brighter and has a longer lifetime due to delayed precipitation.

Radiative forcing (RF) is defined as the instantaneous change in the Earth's radiative flux due to a perturbation in the atmospheric state, e.g., due to a change in greenhouse gas or aerosol concentration (usually compared to pre-industrial conditions). The effective radiative forcing (ERF) additionally accounts for so-called rapid adjustments, which include changes in cloud cover (Boucher et al., 2013). The ERF can be used as a metric when the magnitudes of different anthropogenic forcings are estimated. The ERF due to ACI is estimated to be negative, most likely between -1.2 Wm^{-2} and 0.0 Wm^{-2}, with the best estimate of -0.45 Wm^{-2} (Fig. 2). This high level of uncertainty is due to the large variability between the estimates from measurements and modelling studies, and within different models. Recent cloud scale modelling studies have suggested much lower estimates than global models, which suffer from low resolution (IPCC, 2013). The growing work in fine-scale process modelling, regional scale modelling, and increasing the internal consistency in global models, has led to a better understanding of cloud systems and ACI (IPCC, 2013; Rosenfeld et al., 2014; Bony et al., 2015), but further study of the microphysical processes and their different feedback mechanisms is still crucial for better constraining the RF estimates.

Knowing the exact magnitude of the cooling effect induced by aerosols is of broad interest; not only because it affects the estimates of climate sensitivity from anthropogenic forcing, but also because it can be viewed as a means to prevent or slow down the warming due to increased GHG concentrations in the future. In response to air quality policies, aerosol emission has decreased in developed countries over the past three decades. However, an increase in aerosol emissions has been observed in other areas, especially in Asia (Lu et al., 2011; Kühn et al., 2014). The impact of these changes on the global mean temperature is thought to be small, but it has been argued that a decrease in anthropogenic emissions would suppress the cooling effect, and the warming effect of GHGs would become more dominant.

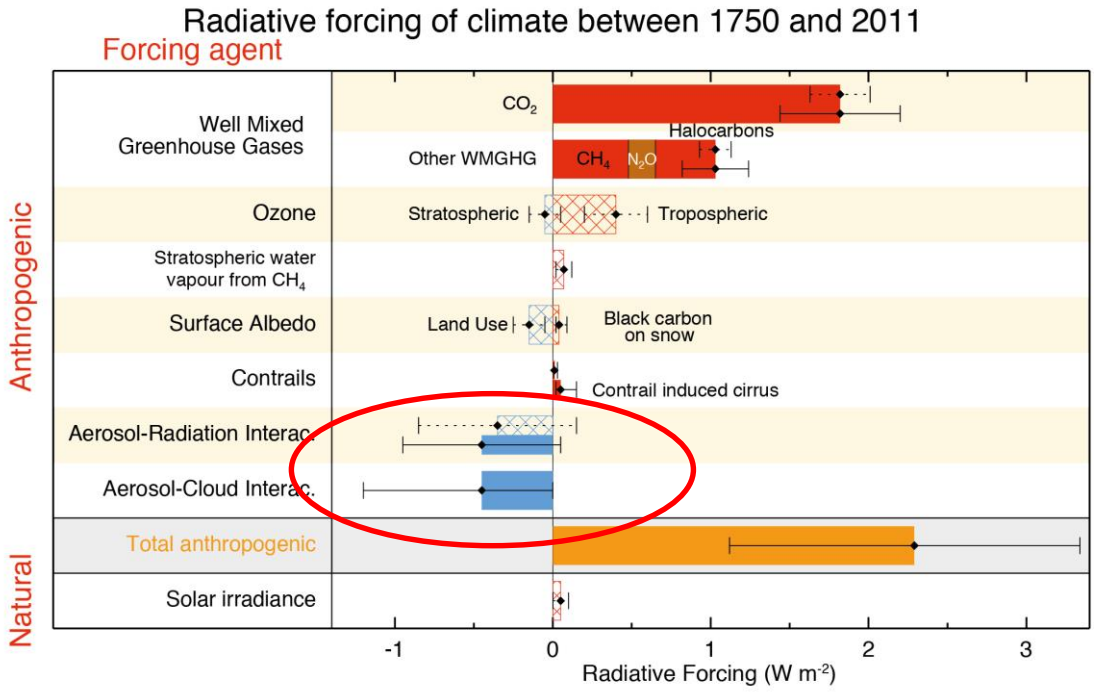

Figure 2: Global mean positive and negative radiative forcings between 1750 and 2011. Estimates of ACI and ARI, highlighted by a red circle (IPCC, 2013).

2.2. Radiation fog

The phenomenon of fog might not be considered as an extreme weather event like storms or tornadoes, or not climatically as important as clouds, but it has a significant effect on daily human life. Fog creates situations where our transportation systems on roads, rails, sea, and air become more vulnerable, requiring specific safety measures to prevent accidents, which lead to delays or cancellations. Financial cost and human loss related to fog events is estimated to be comparable to tornados and storms (Gultepe et al., 2007). Around 35% of all weather-related accidents in the civil aviation sector in the US are attributed to fog events (Herzegh et al., 2004). These cause 168 fatal casualties per year on average.

Fog is defined as a collection of suspended water droplets or ice crystals near the Earth's surface that leads to the reduction of horizontal visibility below 1 km. If the visibility exceeds 1 km, it is classified as mist (Hinds, 1999). There are many different types of fog, which are usually named based on their formation mechanisms. Fog types include radiation fog, advection fog, sea smog, valley fog, etc. In this thesis, we concentrate on radiation fog, which is relatively easy to model with large eddy models, because there is no large scale advection needed to describe the fog formation (**Paper II, Paper III**). The radiation fog life cycle can be divided into three phases: onset, vertical development and dissipation (Fig. 3, Nakanishi, 1999). Radiation fog formation is primarily controlled by the cooling of moist air through longwave radiation and the vertical mixing of heat and moisture, which includes interaction with the land surface. After formation, the development of fog is influenced by longwave cooling and turbulence entrainment-detrainment at the top of the fog, and microphysical processes such as droplet formation and sedimentation. Finally, radiation fog dissipation is driven by shortwave warming of the air and surface, which leads to droplet evaporation both directly and through turbulent mixing.

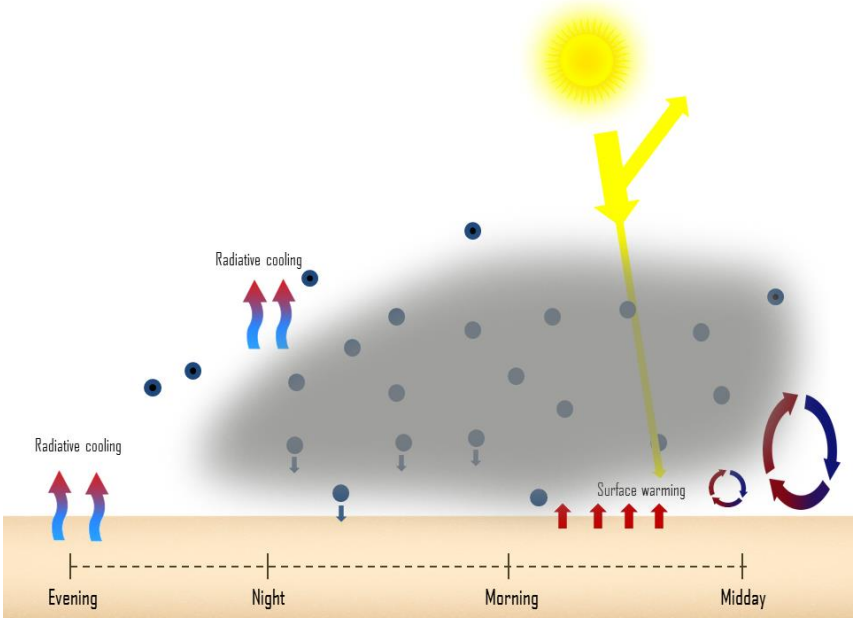

Figure 3: Radiation fog life cycle. The fog is forms and grows vertically during the night, due to radiative cooling of the surface and fog top. The liquid water content in the fog is controlled by droplet sedimentation, and thus, the fog droplet number concentration. After sunrise, the fog starts dissipating due to solar warming of the air and surface, which leads to mixing.

In a similar way as in clouds, aerosol particles act as CCN during the radiation fog life cycle, and have a strong impact on droplet concentrations (Bott et al., 1990; Zhang et al., 2014; Stolaki et al., 2015; **Paper II**). As a higher droplet number concentration means smaller droplet size, an increase in CCN concentration also affects sedimentation and, thus, changes the liquid water content of the fog. Thus, the initial CCN concentration is a key parameter in fog development

(**Paper II**). During the day, absorbing aerosols, such as BC, can warm the air near to the upper layers of the fog, which can lead to the earlier dissipation of the fog (**Paper II**).

The influence that aerosols have on fog through different microphysical processes is recognised as substantial, but poorly understood in many ways (Gultepe et al., 2007). This is due to the very complicated interactions between aerosol particles, fog droplets, and surface meteorology. Over the last few decades, a clear decrease has been observed in fog occurrence throughout Central Europe (Vautard et al., 2009). This has occurred together with improved air quality due to a decreasing trend in sulphur emissions (e.g. Giulianelli et al., 2014). This improvement in air quality is important also from a climatic point of view, as 10-20% of Europe's daytime warming during the mentioned period had been attributed to this reduced frequency in low visibility conditions (Vautard et al., 2009). However, the hypothesis that improvements in air quality have caused the simultaneous reduction in low-visibility (fog) events remains to be verified. This is because so far all of the modelling efforts conducted have lacked several important mechanisms affecting the aerosol-radiation and fog-atmosphere interactions.

2.3. Aerosol-radiation interaction

Atmospheric aerosols can affect the radiative flux by scattering and absorbing radiation (Myhre et al., 2013). Cooling is associated with scattering, and is efficient for aerosol particles with diameters close to the wavelength of visible light (Seinfeld and Pendis, 2006). Absorption produces the opposite effect, i.e. atmospheric warming, and is efficient for all particle sizes. Scattering and absorption are more efficient with incoming shortwave radiation, but large particles, such as dust, also have the ability to influence longwave radiation, although to a lesser extent than clouds or GHGs (Ramanathan and Feng, 2009). Apart from the properties of aerosols, surface properties also strengthen (or weaken) the magnitude of ARI. On reflective or bright surfaces, the cooling effect of aerosol light scattering is usually weaker than over dark surfaces, and vice versa for absorbing particles.

In contrast with the relatively simpler role of scattering aerosols in the atmosphere, absorbing aerosols affect the climate in multiple and opposite ways. Black carbon (BC), dust and brown carbon are the major absorbing aerosol compounds in the atmosphere (Stier et al., 2007). In this thesis, we have studied only the role of BC as an absorbing aerosol, because BC is the most effective absorbing aerosol compound found in the atmosphere (Ramanathan and Carmichael, 2008). The influence of BC on climate is three-fold. First, BC absorbs incoming or reflected (e.g. from snow or clouds) solar radiation, thus warming its surroundings, which can alter the vertical temperature profile, and thus the hydrological cycle near the surface (Bond et al., 2013). Second, the warming due to BC light absorption inside or in the vicinity of clouds or fog layers leads to the evaporation of cloud or fog droplets, causing the semi-direct effect (**Paper II,** Bond et al., 2013). Third, the deposition of BC on reflective surfaces, such as ice or snow, decreases the surface albedo and thus, the amount of reflected light. Furthermore, as darker surfaces absorb more light, deposited BC speeds up ice and snow melt (Law and Stohl, 2007; Ramanathan and Garmichael, 2008; Sand et al., 2013). The ERF due to increased atmospheric BC concentrations from 1750 to 2011 is estimated to be +0.40 (+0.05 to +0.80)

Wm^{-2} (Stocker et al., 2013). Hence, atmospheric BC reduces the negative forcing produced by scattering aerosols. **Paper II** focuses on the semi-direct effect of BC on radiation fog.

As shown in Fig. 2, the net contribution by ARI to RF is cooling, and it is estimated to be −0.45 Wm^{-2} with an uncertainty range from -0.95 to 0.05 Wm^{-2} (Boucher al., 2013). Since there is a large spatial and temporal variation in aerosol properties, the global climate effect of ARI is difficult to assess. Regional forcing has been comparatively well understood, but varies greatly in different regions and in different seasons. Under cloud-free conditions above the ocean, an estimate of RF is negative, but over the polar regions, positive radiative forcing has been observed (Boucher et al., 2013).

2.4. Marine cloud brightening

The increase in anthropogenic greenhouse gas emissions is considered the main reason for the observed global warming. The need for an emission cut has been acknowledged, but due to the slow progress in the reversal of such emission trends, research communities are now looking for other alternatives. Observed negative radiative forcing by the aerosols from volcanic eruptions and observations of ship tracks over oceans gave birth to the idea of controlling or counteracting the effect of GHGs by deliberately increasing aerosol concentrations in the atmosphere, thereby increasing the planetary reflectivity. Such geoengineering methods to counteract global warming through aerosols are termed solar radiation management (SRM) (Shepherd et al., 2009). As of now, these techniques are just proposals and not yet being implemented on a larger scale (Vaughan and Lenton, 2011), but are considered as a potential tool to deal with the current climate change challenge (Irvine et al., 2016; Irvine et al., 2014; Applegate and Keller, 2015). Due to the high coverage and easy accessibility of boundary layer clouds, methods proposing to increase the planetary reflectivity by increasing cloud albedo (aerosol indirect effect) are of considerable interest. One such method, marine cloud brightening (MCB), is considered to have the potential to counteract the warming effect of anthropogenically increased greenhouse gas concentrations.

Stratocumulus clouds are the most dominant cloud type, and cover approximately one-fifth of the Earth's surface (annual mean). Around 80% of all stratocumulus clouds form over the ocean's surface, and they cover 23% of all ocean surfaces (Wood, 2012). Marine stratocumulus clouds (MSC) form usually between 500 - 1000 m above the ocean surface, with a thickness of a few hundred metres. MSC play a crucial role in the global climate system as they effectively reflect the incoming solar radiation above the dark ocean surface, and have a very small impact on the outgoing longwave radiation. Thus, the net radiative effect of MSCs is negative. MSCs are usually characterised by low cloud droplet number concentrations (CDNC). In marine environments, CDNCs in MSCs range from less than 10 cm^{-3} in extremely clean conditions to nearly 50 cm^{-3} above remote oceans (tropic and subtropical regions). Near coastal areas, CDNC is around 200 cm^{-3} or even higher (Wood, 2012). The low CDNC values of MSC over the oceans makes them more sensitive to changes in aerosol concentrations than in polluted conditions. The satellite images of ship tracks (Fig. 4) in some specific meteorological conditions show an optical thickening of the clouds due to aerosol perturbations

below the tracks. The aerosols emitted from the ships' exhausts change the cloud properties through both the Twomey effect and a delay in precipitation formation.

Latham (1990) proposed deliberately increasing the albedo of low level MSCs by injecting sea-salt particles into the air. Offline calculations and global simulations (Latham et al., 2012; Latham et al., 2008) showed that a 0.06 increase in cloud albedo could offset the warming caused by a doubling of atmospheric CO_2 (+3.7 Wm^{-2}, Forster et al., 2007), which, using an

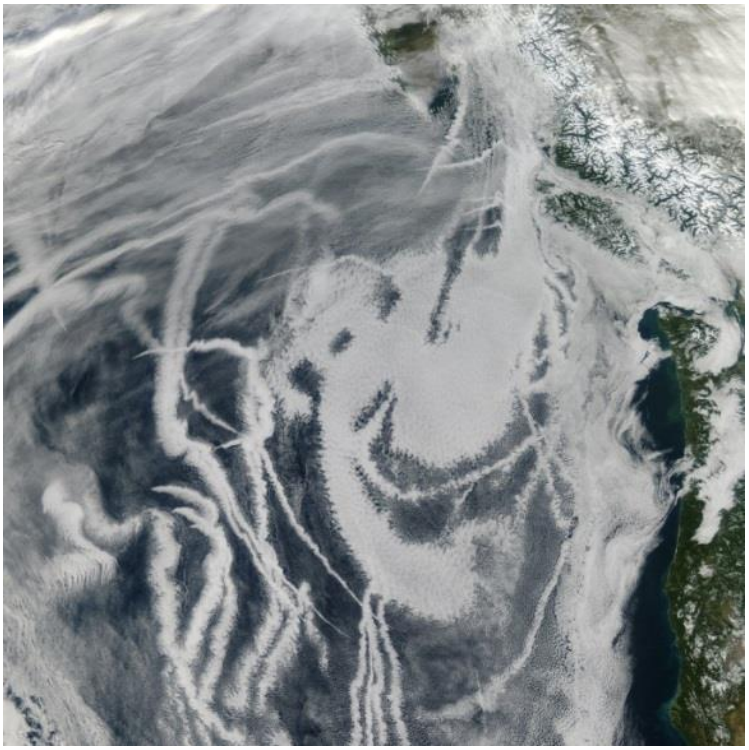

Figure 4: Ship tracks off North America (Photo credit: www.nasa.gov)

emission rate of 1.45 x 106 m^{-1} s^{-1}, would be possible if a uniform CDNC of 375 cm^{-3} over oceans could be achieved. To this end, Salter et al., (2008) proposed the introduction of a fleet of unmanned wind-powered vessels that could inject sea-spray into the air. Since then, many studies using cloud parcel models (Bower et al., 2006), climate models (Jones et al., 2012; Partanen et al., 2012) and cloud resolving models (Jenkins et al., 2013a; Jenkins et al, 2013b; Wang et al., 2011) have been conducted to test the efficacy of this method. However, in global studies, uniform CDNC has been assumed, and in many studies the aerosol removal processes were not included, leading to an overestimation of the achievable albedo change. Korhonen et al., (2010) used a chemical transport model, which takes into account these aerosol processes, and found that the injected particles may suppress the in-cloud supersaturation and prevent existing aerosol particles from forming cloud droplets, thus decreasing the efficacy of the method. Later studies showed that MCB is also sensitive to different regions and aerosol sizes (Alterskjær and Kristjánsson, 2013; Alterskjær et al., 2013). Such results raised questions about the efficacy of the proposed method, and established the importance of detailed aerosol

description in the models (Korhonen et al., 2010; Jones and Haywood, 2012; Alterskjær and Kristjánsson, 2013).

Aerosol injection and cloud processes typically occur at the scale of tens of metres and can only be represented by cloud resolving models. Using a cloud-resolving model, Wang et al., (2011) introduced point source emissions with a similar emission rate as proposed by Salter et al., (2008) at a horizontal resolution of 300 m, and concluded that aerosol-cloud interaction is regime-dependent. In a non-precipitating polluted regime, they achieved a 0.02 increase in cloud albedo and found it difficult to achieve the proposed increase of 0.06 in cloud albedo. Furthermore, Jenkins et al., (2013b) used a large eddy simulation (LES) model and, for the first time, also approximately simulated the liquid water in the injected sea spray. They found that, with the inclusion of water, the aerosol plume height may be notably suppressed. All such results lead to the current understanding that the first published MCB calculations were too simple, and, in order to gain a detailed understanding of the efficacy of MCB, high resolution studies are needed, which also incorporate cloud and aerosol processes as well as transport phenomena.

3. Aerosol Processes

The lifetime of aerosols in the atmospheric boundary layer (ABL) is short, spanning from a few hours to a few weeks. New particles form (or are directly emitted) continuously in the atmosphere, grow, and transform chemically before being removed from the atmosphere. This section discusses the main aerosol microphysical processes that significantly affect the aerosols themselves, and also their interaction with the atmosphere.

It is best to characterise aerosols by their population instead of individual particles, because the particle number and properties are extremely variable in space and time. The aerosol size distribution, chemical composition, and shape of the particles are the most important aerosol characteristics. Aerosols are usually classified according to their size, diameter 'd_p', into four or five distinct modes, which usually follow lognormal distributions (Hewitt and Jackson, 2009). If five modes are used, the first one is the cluster mode, which consists of small clusters of molecules with diameters less than 2 nm. The cluster mode is followed by the nucleation mode, with particle sizes between 2 to 30 nm. The nucleation mode has the smallest mass concentration, but can contain the highest number of particles. New particles form and grow mainly through condensation in the nucleation mode. The particle number in the nucleation mode can also decrease through coagulation with larger particles. The third mode is the Aitken mode, which contains particles between 25 nm and 100 nm in diameter. These particles are large enough to become climatically relevant in humid conditions, where they grow due to water uptake. Next is the accumulation mode, with particle sizes ranging from 100 nm to 1 µm (Seinfeld and Pandis, 2006). Aitken and accumulation modes are the most persistent in the atmosphere because all removal processes are slow for particles around 100 nm. Particles in the accumulation mode take part in cloud formation and also interact with shortwave (SW) radiation directly. Aerosol particles greater than 1 µm belong to the coarse mode (Hewitt and Jackson, 2009). The upper limit of this mode (normally considered to be 10 µm) is determined by the gravitational force. The coarse mode contains particles like sea-salts, volcanic ash, pollen, and mineral dust. Because of the large particle size, the coarse mode has a high aerosol mass concentration, but due to efficient gravitational settling, the aerosol number concentration is low.

3.1. Particle origin in the atmosphere

Aerosols are classified in several ways according to their source. The most common classification of aerosols is into primary and secondary aerosols. Particles that are emitted directly into the atmosphere as a result of wind friction, incomplete combustion, mechanical processes or from volcanic eruptions are classified as primary aerosols. Secondary aerosols form in the atmosphere from gas-phase species (aerosols precursors). These gas-phase species, after undergoing chemical transformation, condense to form additional aerosol mass through condensation, or to form new particles through nucleation. The second important classification of aerosols according to their source is into natural and anthropogenic aerosols. Natural sources contain aerosols that are emitted into the atmosphere from oceans, vegetation, fires and

volcanoes. Aerosols that are emitted into the atmosphere as a result of human activity are termed anthropogenic aerosols. Anthropogenic aerosols are emitted from sources like the combustion of fossil fuel and biofuel, industrial activities, transportation, and cooking related activities. Beyond these, there are also some other classifications of aerosols, such as urban, marine or continental aerosols, tropospheric or stratospheric aerosols.

In marine environments, sea spray drops are released into the air from breaking waves and related bubble-bursts, causing the particle flux to be wind dependent. Sea-salt particles are coarse mode particles with dry sizes that typically range between 0.01 and 10 μm (Clarke et al., 2003). Normally, the largest particles fall back into the water and therefore are not climatically important. Some studies have also shown that very large particles, i.e. up to 17 μm, may participate in warm rain formation (Jensen and Lee, 2008). On continental surfaces, wind friction causes dust particles to be lifted into the air. The amount of lifting depends on the wind speed and particle mass. The main sources of dust particles on the global scale are deserts and arid regions. Normally dust particles (or mineral dust particles) are larger than 1 μm in diameter, and thus are predominantly coarse mode particles. Aerosol particles from volcanic eruptions (also called volcanic ash) contain fragments of pulverised rocks and minerals of sizes ranging from micrometres to millimetres. Volcanoes also emit sulphur rich gases (Sulphur dioxide, SO_2, and hydrogen sulphide, H_2S) that oxidise in the atmosphere to form sulphate aerosols. Depending on the intensity and altitude of the volcanic eruption, aerosol particles and gases can be transported up to thousands of kilometres and, if they reach the stratosphere, they can persist up to years. Other important primary and natural aerosols are biogenic aerosols. They are comprised of plant and insect debris, pollen, spores, bacteria and viruses. These are also coarse mode particles, with sizes up to hundreds of micrometres. Seawater may also contain biogenic matter, which can also be transported into the atmosphere along with sea-salts.

Biomass burning is the intentional burning of forests, woodlands and agricultural lands. Forest fires are natural fires caused predominantly by lightning, but about 90% of fires involve biomass burning (Jacobson, 2005). Emissions from biomass burning include CO_2, CO, NO_x, CH_4, non-methane hydrocarbon and organic particulate matter. The quantity and type of emissions from biomass burning depends on the type of land and meteorological conditions, like moisture content, ambient temperature, humidity and wind speed. Because of the presence of absorbing aerosols, biomass emissions have a critical impact on the climate. It is thought that not only do biomass emissions have a direct effect on the climate by the absorption of incoming solar radiation, but they also affect the climate indirectly by burning off the clouds (Jacobson et al., 2014; **Paper II**). Other important anthropogenic sources include biofuel and fossil fuel burning.

Major secondary aerosols arise from precursor gases like sulphur dioxide, nitrogen oxides (NO_x), ammonia (NH_3) and organic compounds with different volatilities. The most important condensing gas is sulphuric acid (H_2SO_4), which is produced in the atmosphere by the oxidation of sulphur dioxide (SO_2) emitted from fossil fuel combustion, volcanoes, biomass burning, or from dimethylsulphate (DMS) emitted from oceans. H_2SO_4 condenses under all atmospheric conditions to pre-existing particles to form aqueous sulphate particles, or it can nucleate

homogeneously to form new particles. The composition of these sulphate particles can then be modified by the condensation of other gases like NH_3, HNO_3, and organic compounds. Recently, how the chemical transformation of atmospheric organic compounds results in the formation of secondary organic aerosols (SOA) has been also widely studied. The formation and evolution of SOA properties is still largely unknown. The most studied formation mechanism of SOA is through the oxidation of volatile organic compounds (VOCs). SOA is thought to contribute the majority of organic aerosol (OA) mass in the atmosphere. Current research shows that about 90% of SOA is formed from biogenic VOCs (Ehn et al., 2014; Tsigaridis et al., 2014).

Figure 5: Schematic diagram showing some of the aerosol sources and aerosol processes in the atmosphere

3.2. Particle growth mechanisms

In order to survive the scavenging mechanisms and become climatically relevant (to act as CCN and interact with radiation), freshly formed particles in the nucleation mode need to grow (Kerminen et al., 2012). **Condensation** is the main particle growth mechanism in the atmosphere. Due to condensation, particles grow from nucleation mode to Aitken mode, and if there is enough condensable material, the growth continues up to the accumulation mode. Thus, particle growth results in the increase of the particle number concentrations in both the Aitken and accumulation modes. Sulphuric acid (H_2SO_4) has been identified as a key component responsible for the particle growth in the early stages (Sipilä et al., 2010). However, other compounds such as ammonia, amines and low-volatile organics can also condense on newly formed particles (Kirkby et al., 2011; Almeida et al., 2013; Kulmala et al., 2014). After the

initial growth, nitrates and semi volatile organics can also be responsible for particle growth towards the accumulation mode (Riipinen et al., 2012; Schobesberger et al., 2013).

Condensation occurs when more vapour molecules arrive at the particle's surface than leave it. This results in the net growth of the particle. The opposite process is called evaporation. Condensation/evaporation is driven by the difference between the vapour pressure (or molecular concentration) at the droplet surface, $P_s(C_s)$, and the vapour pressure (concentration) far away from the droplet, $P_\infty(C_\infty)$. The relation between the rate of the diameter change (dd_p/dt) and the concentration difference $(C_\infty - C_s)$ in the case of assuming spherical particles can be given as (Seinfeld and Pandis, 2006):

$$\frac{dd_p}{dt} = \frac{4\, D_i\, M\, \beta_M\, (C_\infty - C_s)}{\rho\, d_p} \qquad (1)$$

Here d_p is the particle diameter, D_i is the binary diffusion coefficient in air for the condensing vapour, M is the molecular mass of the condensing vapour, and ρ is the mass density of the condensed molecules. β_M is the transitional correction factor, which was introduced to account for the difference in the condensation fluxes at small and large aerosol sizes.

The saturation vapour pressure is defined as equilibrium vapour pressure over a macroscopic (plane) surface. If the liquid surface is curved, the partial pressure required to maintain equilibrium is always higher relative to the plane surface of the same composition. This phenomenon is called the Kelvin effect and is expressed in the form of a correction factor, Ke, which is determined at a given temperature (T) by

$$Ke = \frac{p_s(T, d_p)}{p_s(T, d_p = \infty)} = \exp\left(\frac{4\,\sigma\, M}{\rho\, R\, T\, d_p}\right), \qquad (2)$$

where σ is the surface tension, M is the molecular mass of the vapour, and R is the ideal gas constant.

In the atmosphere, particle motion is driven either by Brownian motion or by some external forces like gravitational settling, turbulence, or electrostatic force (Seinfeld and Pandis, 2006). While moving through the air, the particles collide and stick (or 'fuse' in the case of liquid spheres) to each other, forming larger particles in the process. This process is termed **coagulation**. Coagulation reduces the number concentration of the particles in the atmosphere, but it conserves their total aerosol mass.

In accordance with the process that drives particle collision, coagulation is further sub-termed Brownian coagulation (due to Brownian motion) or kinematic coagulation (motion due to external forces) (Jacobson, 2005). In this thesis, mainly Brownian coagulation and coagulation due to gravitational settling are considered. The coagulation rate depends on the particle collision rate and number concentration. The collision rate between particles is defined by the Knudsen number Kn in air (Jacobson, 2005),

$$Kn = \frac{2\lambda}{d_p}, \qquad (3)$$

where λ is the mean free path of a particle. For $Kn \ll 1$, the Brownian coagulation coefficient is limited by the diffusion of particles (continuum regime) (Jacobson, 2005). When colliding with each other, for particles i and j in the continuum regime, with sizes r_i and r_j respectively, the coagulation coefficient is given as

$$K_{ij} = 4\,\pi\,(r_i + r_j)(D_i + D_j)\ , \tag{4}$$

where $D_{i,j}$ are the diffusion coefficients of the two particles, respectively. For $Kn \gg 1$, the kinetic theory of gases holds and the particles are assumed to be in the free molecular regime. In this case, the coagulation coefficient is given as:

$$K_{ij} = \pi(r_i + r_j)^2\sqrt{(v_i^2 + v_j^2)}\,, \tag{5}$$

where $v = \sqrt{8k_B T/\pi m}$ is the thermal speed of the particle of mass m in air and k_B is Bolzmann's constant. If $Kn \approx 1$, particles are in the transition regime and the coagulation coefficient is calculated by the interpolation methods derived by Fuchs (1964).

It follows from the equations above that Brownian coagulation is at its most efficient between different sized particles. Large particles, because of their large surface area, 'capture' the small, fast-moving particles. Particles of similar sizes have a low coagulation rate. It is less likely for large particles to collide with each other because of their slow motion, while small but fast moving particles have a low probability of colliding because of their small surface area. Overall, Brownian motion is the main mechanism for nucleation mode particle scavenging in the atmosphere (Pierce and Adams, 2007). The coagulation coefficient in the case of gravitational coagulation is given as:

$$K_{ij} = E_{coll,ij}\,\pi(r_i + r_j)^2\ |V_i - V_j|\ , \tag{6}$$

where E_{coll} is called the collision efficiency, which gives the ratio between the total number of collisions between particles and the number of particles in an area equal to droplet's effective cross sectional area (Seinfeld and Pandis, 2006). $V_{i,j}$ are the terminal settling velocities of the particles, respectively. Gravitational coagulation is high in cases of very large collectors, like cloud droplets, sea spray or soil dust particles (Jacobson, 2005).

Both coagulation and condensation processes act more efficiently in clouds, where cloud droplets with sizes of several micrometres provide a much larger surface area and volume for aqueous phase chemical reactions than aerosol particles in subsaturated conditions. This is called the **cloud processing** of aerosol, changing the properties of aerosol particles in several ways as the aerosol is cycled through the cloud. The condensation of different chemical species can lead to aqueous phase chemical reactions, producing non-volatile mass that remains in the aerosol phase even after water evaporation. This can lead to a bimodal aerosol size distribution, where the particles in the accumulation mode grow larger. The conversion of SO_2 to sulphate in cloud droplets is the best-known example of such a process. Thus, cloud processing not only changes the size distribution of aerosols, but also affects the chemical composition of aerosols. Further, cloud droplets also enhance the loss of small particles via collision-coalescence (or coagulation), which leads to the growth of particles in the accumulation mode. Thus, not only do the aerosols change the cloud droplet properties, but the clouds also modify aerosol

properties, and this cloud processing of aerosols has important implications for aerosol-cloud interactions.

3.3. Cloud droplet activation

Clouds are formed when the air parcel cools and the relative humidity (RH) exceeds 100% (or, equally, the water saturation ratio S exceeds 1). Under such supersaturated conditions, water vapour quickly condenses to form cloud droplets. In an atmosphere without aerosol particles, water vapour would require highly supersaturated (SS = (S-1)*100 %) conditions (RH > 400%) in order to form cloud droplets through homogenous nucleation. In actual atmospheric conditions, water condenses on some available surface, which acts as a seed for cloud droplet formation. Aerosol particles, which are able to act as such a seed, are termed cloud condensation nuclei (CCN). Cloud droplet activation is described by the Köhler theory, which explains the equilibrium between the liquid phase of the aerosol particle and water vapour. Köhler theory is a combination of two processes, Kelvin effect and Raoult's law, and is given as

$$S_{\mathrm{eq}} = \mathrm{a_w} \exp\left(\frac{4\, M_{\mathrm{w}}\, \sigma}{\rho\, R\, T\, d_{wet}}\right) , \tag{7}$$

where S_{eq} is the equilibrium saturation ratio, $\mathrm{a_w}$ is the water activity of the solute, M_{w} is the molar mass of water, σ is the surface tension, ρ is the density of the solution, and d_{wet} is the particle wet diameter. The exponential term in eq. 6 is the Kelvin effect (as explained in section 3.2), which accounts for the increase in vapour pressure due to the curvature of the droplet surface. Raoult's law, considering the influence from solutes, tends to decrease the water vapour pressure:

$$\mathrm{a_w} = \gamma \left(\frac{n_w}{n_w + i n_S}\right) . \tag{8}$$

Here $\mathrm{a_w}$ is the activity of water, n_{w} and n_S are the number of moles of water and solute in the solution, respectively, i is the dissociation factor of solute (e.g. the number of ions formed from the salt molecule), and γ is the activity coefficient of water, which accounts for the non-ideality of the solution. The more dilute the solution, the more ideal it becomes, and the more γ will approach 1.

Köhler theory explains the relationship between saturation ratio and particle size. The critical saturation ratio (S_c), which depends on the particle dry size and composition, can be calculated by calculating S_{eq} as a function of droplet diameter and finding the maximum of the curve. It tells us the ability of a particle to activate if the maximum supersaturation (S_{max}) for the cloud formation is known. The particle can activate into a cloud droplet if $S_c < S_{max}$. Thus, the CCN concentration is actually a function of supersaturation, CCN(SS), giving the potential number of droplets formed at a certain supersaturation. The wet diameter at which the equilibrium saturation ratio is at a maximum is termed the critical diameter.

What controls the maximum supersaturation in the cloud is competition between the air parcel cooling (increasing the supersaturation) and the condensation of water on droplets (decreasing

the supersaturation). The maximum supersaturation at the cloud base is usually achieved when these are of the same magnitude. In the case of clouds, the cooling is caused by the updraft motion of air parcels, and thus it is the main parameter controlling which particles of all the CCN available will actually form cloud droplets. The most sophisticated parameterizations for cloud droplet number concentration usually solve the maximum supersaturation as a function of updraft and aerosol present, and then use the Köhler theory to estimate which particles activate as cloud droplets (e.g., Pruppacher and Klett 1978, Abdul-Razzak et al., 2002, Nenes et al., 2003). As the atmospheric aerosol is chemically complex, numerical models often parameterize the aerosol hygroscopic properties. A commonly used parameterization by Petter and Kreidenweis, (2007) introduces the hygroscopicity parameter κ to represent a quantitative measure of the water uptake characteristics of different aerosol chemical components, and thus CCN activity.

It depends on the conditions whether the number of available CCN or the updraft velocity is more important for cloud droplet number concentration (McFiggans et al., 2006, Reutter et al., 2009). Usually, in cases with low total CCN, droplet activation is limited by CCN availability, even with high updraft velocities. With high CCN concentrations, it is commonly observed that an increase in total CCN no longer increases the droplet concentration, and thus, it is mainly the updraft velocity that controls droplet activation.

3.4. Aerosol removal processes

Dry and wet deposition are the ultimate processes by which particles are removed from the atmosphere. There are a number of factors that affect the deposition process, like the size and shape of the particles, chemical composition, turbulence close to the surface, the amount of precipitation, and surface type (Jacobson, 2005; Seinfeld and Pandis, 2006). **Dry deposition** removes the particles from the atmosphere in the absence of precipitation. It occurs when a particle comes into contact with a surface and sticks to or is absorbed by it. Particle properties like size, density, and shape determine the rate of capture by the surface. In addition to that, the surface type is also very important. For instance, the rate of deposition on smooth surfaces (like ice) is lower than on rough surfaces (like vegetated land). There are different mechanisms affecting particle removal in the vicinity of a surface; the most important are Brownian diffusion, impaction and interception (Seinfeld and Pandis, 2006)

For small particles, impaction and turbulence are the dominant transport mechanisms, but when aerosols grow large enough (coarse mode) they fall in the atmosphere due to gravity. This sinking of large particles due to gravitational fall velocity is termed as **sedimentation** (Jacobson, 2005). Coarse mode particles, like sea-salt and dust particles, are efficiently removed from the atmosphere by sedimentation. Dry deposition is slow in accumulation mode particles because of their relatively low fall speed and sizes small enough to follow the streamlines to avoid impaction.

The dry deposition flux is directly proportional to the concentration C of the particles above the surface (Seinfeld and Pandis, 2006). The dry deposition flux is calculated as:

$$F = -v_{\mathrm{d}}C \tag{9}$$

where v_d is the deposition velocity, which depends on a variety of physical and chemical processes. v_d is used as a single parameter to determine the deposition flux, but it incorporates several different processes. There are three distinct steps involved in dry deposition: (1) the transport of particles from the atmosphere to the thin layer of air adjacent to the surface (typically 10 cm), (2) the transport of particles across this layer to the surface through molecular diffusion and (3) the surface uptake of the particles (Jacobson, 2005). Deposition velocity is generally parameterized by taking into account the above three steps as resistances, and calculated as a reciprocal of the sum of the different resistances. For the deposition velocity, several parameterizations are available, such as Walcek et al., 1987, Russel et al., 1993 and Zhang et al., 2001.

Wet deposition is the dominant removal process in precipitating regions. The scavenging of aerosol particles and soluble gases from the atmosphere through precipitation (Cloud, fog, rain, ice etc.) is termed wet deposition (Seinfeld and Pandis, 2006). The effectiveness of wet deposition depends on the type and intensity of the precipitation and on the particle number concentration and chemical properties (e.g. hydrophilic or hydrophobic) of the particle.

The wet deposition process can be divided into in-cloud and below-cloud scavenging. When aerosols are inside a cloud, they can act as cloud condensation nuclei (CCN) or ice nuclei (IN) and form cloud droplets. A fraction of the cloud droplets (or ice crystals) grow large enough to form precipitation, which results in the effective removal of particles from the atmosphere. This process is termed in-cloud scavenging or rainout. Aerosols between 0.08-1 μm efficiently participate as CCN (Croft et al., 2010) and thus their number concentration is affected by rainout. Aerosol mass is primarily scavenged by rainout for hydrophilic ("water loving") aerosols. Cloud droplets that do not grow into rain droplets eventually evaporate to re-form aerosol particles, which might have different chemical properties than the original CCN due to the chemical reactions that took place inside the cloud droplet. Smaller aerosol particles with diameters less than 0.01 μm, which are inside the cloud but do not act as CCN, are quickly scavenged by cloud droplets (or ice crystals) through impaction.

Particles located below the cloud base can be swept out by falling hydrometeors (rain or snow). This wet deposition process is called below-cloud scavenging or washout. It is efficient in removing very small and very large particles, for the reasons mentioned in the coagulation discussion. For particles with diameters between 0.01μm and a few micrometres, the below-cloud scavenging rate can be several orders of magnitude smaller (Feng et al, 2007).

3.5. Aerosol effect on cloud dynamics

Cloud microphysical processes are closely linked with cloud thermodynamics, and thus affect cloud dynamics. To complicate the aerosol-cloud interaction puzzle, the clouds also feed back to the aerosol properties. A cloud droplet, right after its inception, will grow first by condensation to the size at which collisions and coalescence become fast enough to modify the droplet population. At that point, the droplet has a size of around 50 μm, after which its sedimentation velocity increases quickly as a function of size, and drizzle is formed. A drizzle-sized droplet still follows air updrafts, collides with smaller droplets and grows in size. After a

while, the droplet may grow so large that its fall velocity becomes greater than the updraft and it thus falls back to the cloud base level. Once below cloud base, it depends on the droplet size and vertical profile of RH to determine whether it is large enough to survive below cloud evaporation and can reach the surface as precipitation. Aerosols can modify this process by increasing the amount of droplets, thus decreasing the mean size, which will delay the formation of drizzle and precipitation. Because of that, a longer time is needed for precipitation to form, and in some cases this can be observed as an increase in the cloud liquid water content and height (Fig. 1). On the other hand, precipitation is an efficient way to remove aerosol particles from the atmosphere (as discussed in the previous section). Thus, it reduces the particle number concentration in the atmosphere, which, in turn, affects cloud formation, as a lower particle concentration leads to bigger cloud droplets (Fig. 1).

The picture becomes even more complicated if cold cloud (where the cloud top temperature is < 0C) processes are taken into account. Cold clouds contain ice particles and, like the formation of cloud droplets, the formation of ice particles requires aerosols as seeds, which are called ice nuclei (IN). Unfortunately, the general understanding of the aerosol indirect effect on cold clouds is still fairly poor. The complications in understanding the aerosol effect on cold cloud processes involves determining the ice fraction of a cloud, size, shape and ice water content. Aerosols affect these mentioned properties but the extent of the effect is still not well understood (Lohmann and Feichter, 2005). Another important factor is the number of freezing processes that can initiate the ice formation. Unlike in the case of warm clouds, where vapours need the aid of CCN to condense, in cold clouds, ice crystals can form by freezing cloud droplets (below -40C), i.e. without the aid of IN. However, ice nuclei are beyond our scope, as this thesis only focuses on warm clouds.

4. Modelling tools

Most of our understanding of the atmospheric boundary layer (ABL) comes from observation (e.g. remote sensing, satellite or sensors). In the real world, it is not possible to observe any atmospheric process in isolation, as different processes happen and interact at the same time. Numerical models provide us with a platform to study the ABL under controlled conditions, and to perform sensitivity analyses of any particular processes or phenomena in isolation from the rest of the processes. Numerical models can be used together with observational data to test different research hypotheses. It would not be wrong to say that only the agreement of the modelling and observational data indicates that a correct understanding of the respective phenomenon has been developed.

The horizontal domain of a model is either global or regional (covering only part of the Earth), with boundary conditions derived from a global model. Regional models allow for the use of high resolution (finer grid spacing) than global models, because the available computational resources are focused on a specific area instead of being spread over the globe. When smaller scale phenomena that are not specific to any geographical location are studied, idealised model setups are usually used. Over the past decades, high-resolution large eddy simulation (LES) models have emerged as very useful tools in the field of atmospheric sciences. Turbulent flows tend to differ from one another in their large eddy structure, while small scales in turbulent flows tend to be statistically similar. The LES approach uses this philosophy by explicitly resolving the large energy containing eddies and parameterizing the less crucial small-scale eddies (Argyropoulos and Markatos, 2015). The influence of eddies on cloud formation and other processes is therefore also directly simulated in LES studies.

LES models have been successfully used in boundary layer cloud studies, for example: non-precipitating and precipitating shallow cumulus (Siebesma et al., 2003; Van Zenten et al., 2011) and stratocumulus clouds (Moeng et al., 1996; Stevens et al., 2005; Ackerman et al., 2009); sheared and stable boundary layers (Holtslag, 2006; Beare, 2006); radiation effect (Pincus et al., 2013); and the diurnal cycle of cumulus clouds (Brown et al., 2002). LES has also seen success in industrial applications (Fureby, 2008). In applications where very detailed information on turbulence is needed, the solution can be provided through direct numerical simulation (DNS) models. DNS provides an accurate numerical solution to the three-dimensional Navier Stokes equation, without the need for a parametric turbulence model. It is the most straightforward and accurate approach to solve turbulent flows, but also computationally highly demanding, and thus only applicable for small simulation domains. Lately, DNS has been used, for example, to study the mixing of air at cloud edges (Andrejczuk et al., 2006).

Although it is possible with LES models to study atmospheric flows down to metre scales, it is not always computationally feasible to represent all of the sub-micrometre scale processes acting on aerosol and cloud droplets with such a high amount of detail. The major challenge in modelling aerosol-cloud interaction is the representation of cloud activation and its sensitivity to aerosols and dynamic parameters. Representing the aerosol size distribution and chemical

composition accurately would require several hundreds, or even thousands, of variables, and thus, resolving aerosol-cloud processes at that level in cloud-resolving simulations is in practice out of computational range. In order to limit the computational cost, aerosol particle size and composition still need to be heavily discretised depending on the model application (**Paper I**, **II**, **III, IV**). Thus, highly detailed 0-dimensional models are usually used to study aerosol microphysics and detailed chemistry. Using such models, it is possible to study in detail how, for example, aerosol chemical composition and related particle phase thermodynamics affect the droplet formation.

In this thesis, different modelling approaches have been used to study aerosol-cloud interaction at the microphysical and cloud resolving scale. In **Paper I**, **II**, and **III,** the large eddy model UCLALES has been used, and in **Paper IV**, a cloud parcel model is employed. This chapter presents a brief description of the models used in this thesis.

4.1. UCLALES

UCLALES (Stevens et al., 2005) is a LES model that has been designed to study convective boundary layers with shallow cumulus and stratocumulus clouds. In the standard model distribution, a two-moment warm-rain microphysical scheme (Seifert and Beheng, 2006) is implemented (Stevens and Seifert, 2008). This scheme assumes cloud droplets with a fixed (user-specified) number concentration. Cloud (or rain) droplets are defined as liquid condensate with appreciable fall velocities, and are allowed to evolve under the action of the ambient flow and microphysical processes (auto-conversion, accretion, self-collection, sedimentation). To take into account the condensation of water, a saturation adjustment scheme is implemented in the model. This scheme diagnoses the cloud mass concentration as the difference between total water and liquid water saturation mixing ratio. Thus, the actual activation or evaporation processes are not accounted for.

The model enforces the surface by either free slip or no-slip boundary conditions on the grid-scale tangential velocities, with free-slip being the default. The model supports different methodologies for specifying the heat fluxes at the lower boundary (surface). They can be prescribed or calculated based on the prescribed gradients or prescribed surface properties. The grid is doubly periodic (in x-y) and bounded in the vertical, z. The vertical is spanned by a stretchable grid and the horizontal is tiled by uniform squares. A sponge layer is applied to the domain top in order to damp the spurious gravity waves. This artificial sponge layer prevents the gravity waves from being reflected at the top boundary.

In UCLALES, atmospheric radiation can be prescribed or calculated during the simulation. For the calculation of radiative transfer, a delta-four-stream radiative transfer scheme is used (Fu and Liou, 1993). The scheme takes into account atmospheric gases and clouds, with the total droplet number concentration and cloud water as an input. Further, a Monte Carlo spectral integration is implemented in the default scheme to reduce the computational burden (Pincus and Stevens, 2009).

4.2. SALSA aerosol module and its cloud extension

In order to represent aerosols in UCLALES, we use the sectional aerosol module SALSA (Kokkola et al., 2008). It is used to calculate the microphysical processes of nucleation, condensation, coagulation, cloud activation, sulphate production, and hydration. SALSA's bin setup is shown in Fig. 6. In its standard setup, SALSA uses 10 size bins to represent the aerosol size distribution, with two parallel populations (external mixing), which constitutes a total of 17 size bins. In addition, the aerosol population is divided into 2 logarithmically spaced sub-ranges (numbered 1 and 2) with 3 bins in the first and 7 bins in the second sub-range. SALSA is designed to be flexible and allows for easy modification in the amount of size bins, sub-ranges, and externally mixed populations. To reduce the computational burden of the module, only the most (globally) relevant chemical compounds and microphysical processes are included for each size range. Sub-range 1 contains 3 bins with average diameters ranging from 3 nm to 50 nm and contains only organic carbon and sulphates. Particles in this sub-range are assumed to be internally mixed, and the only active processes are condensation and coagulation. Sub-range 2 consists of 7 bins with particle diameters ranging from 50 nm to 10 µm. In this sub-range, the model assumes that particles are externally mixed and thus, defines a soluble (2a) and an insoluble (2b) population. 2a contains organic carbon (OC), sulphates (Su), sea-salts (SS), black carbon (BC) and mineral dust (Du), and 2b consist of OC, Su, BC and Du. Particles of sub-range 2 are sensitive to all aerosol processes and can also participate in cloud activation. Additionally, each size bin includes information on the number concentration (N) of the particles it contains. SALSA does not restrict the shape of the size distribution, making it possible to simulate both tropospheric and stratospheric aerosols. Further details of the aerosol bins can be found in Laakso et al., 2016.

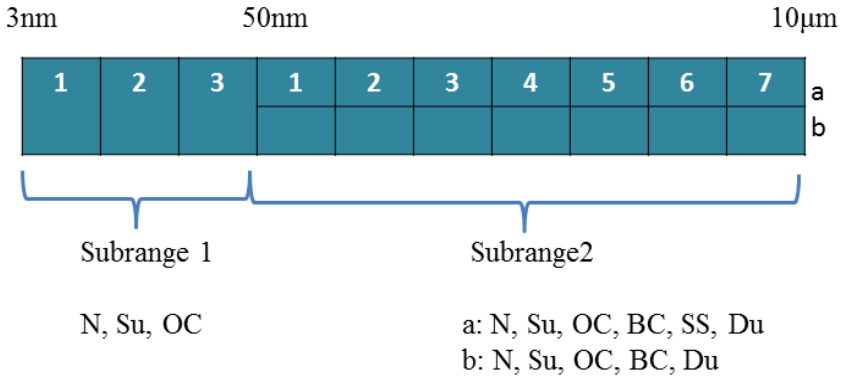

Figure 6: Schematic of SALSA parallel size bin layout.

In the new cloud-extended SALSA, additional size sections for cloud droplets and drizzle are implemented, as shown in Fig. 7. As a compromise between accuracy and computational burden, we defined cloud droplet and precipitation droplet bins (within the SALSA framework) to be parallel to the aerosol bins (specifically, the 2a/b-bins by default) in terms of the dry diameter of the activated cloud condensation nucleus (CCN). In this way, the properties of the

aerosol size distribution are preserved upon cloud droplet activation, as well as the evaporation of cloud droplets. The drizzle size bins range from 50 µm to 2 mm constituting 7 size bins, and here the wet size of particles was followed for the accurate simulation of precipitation. The cloud droplets that grew large enough were moved from cloud bins to the first bin of the drizzle classes using an auto-conversion routine. The spectral resolution given by this bin layout is quite coarse, but does provide a good compromise between computational cost and model performance. A detailed description of the methods for solving aerosol microphysical processes is given by (Kokkola et al., 2008, **Paper III**).

The evaporation and deactivation of cloud droplets was accounted for through the resolved condensation, upon which the activated aerosol particles were released back to the aerosol bin regime as illustrated in Fig. 7. For this to take place, a very simple diagnostic is used, where sub-saturation with respect to water vapour is required and the cloud droplet diameter should be 50 % of the critical diameter dictated by the properties of the CCN (or 2 µm at maximum). These thresholds were obtained by physical reasoning and through experimentation with the model.

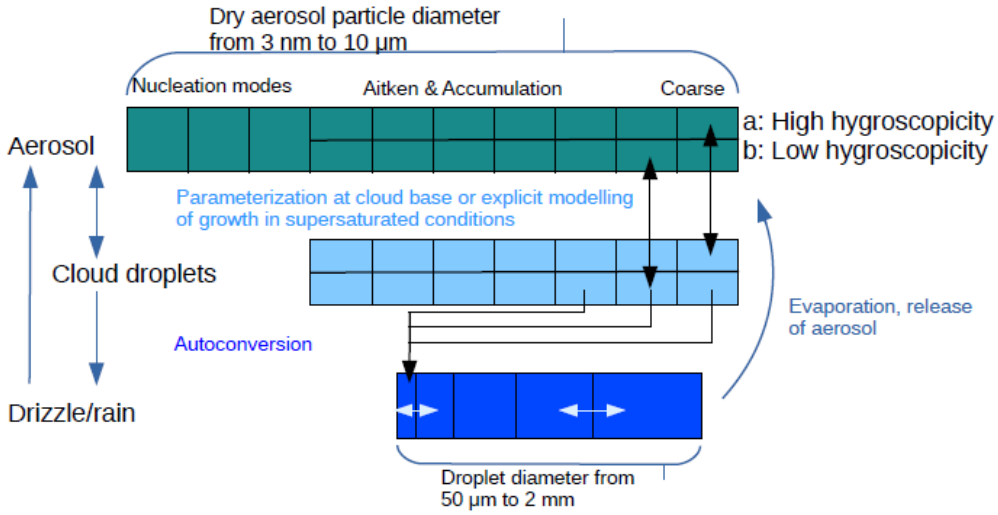

Figure 7: A schematic of the parallel bin layout of extended SALSA, also showing the cloud droplet and precipitation drops bins (From **Paper III**).

To reduce the computational cost during the simulations for this thesis, we neglected some aerosol types from SALSA and defined only sulphate (**Paper I**, **II** and **III**), sea-salt (**Paper I** only) and black carbon (**Paper II** only). Different setups were used for the aerosol microphysics in different studies. **Paper I** considers only Brownian coagulation, and from other processes, only water condensation and the dry deposition of particles are considered. In **Paper II,** the sedimentation and deposition of cloud droplets are assumed, and processes affecting aerosol concentration are neglected. **Paper III** includes most of the processes related to aerosol cloud interactions that are described in earlier sections. In **Paper IV,** aerosol

condensational growth is considered in detail, but other processes are omitted. The reasoning behind these choices is presented in the closer introductions of the different papers.

4.3. Cloud parcel model

The cloud parcel model (CPM) we used in our study is a zero dimensional aerosol model designed to study the evolution of the physical and chemical properties in an aerosol population through cloud cycles. It is a sectional model in which dry size sections are defined using a constant volume ratio between adjacent sections, and sections are allowed to move freely in diameter space during water condensation and evaporation. The model includes options for the following aerosol processes: condensation/evaporation, coagulation/chemical reactions in the liquid phase, adiabatic processes and the emissions of gas phase species. The adiabatic equations include differential equations for total pressure, air temperature and the altitude of the air parcel. The model also includes modules for equilibrating the aerosol population with water vapour and trace gases, and for calculating the optical properties of the aerosol population. Further details of the model can be found in Kokkola et al., (2003a).

Beyond using the model in adiabatic mode, it can be also forced with air parcel trajectories (Romakkaniemi et al., 2005, 2009; **Paper IV**). The CPM does not represent the dynamics related to cloud formation or the mixing of different air parcels. Thus, any cloud resolving model or large eddy model can be used to simulate the boundary layer dynamics and to obtain a set of air parcel trajectories under those conditions. The CPM uses these trajectories to simulate aerosol/cloud microphysics in the air parcel as it moves along the trajectory path.

4.4. PALM

The PArallelized LES Model (PALM) was developed at Leibniz University, Hannover (Raasch et al., 2001; Maronga et al., 2015), Germany, and has been successfully applied for a variety of boundary layer research questions related to turbulence both in the atmospheric and oceanic boundary layer (e.g. Maronga et al., 2013; Park et al., 2013). The model is highly optimised for use on massively parallel computers with distributed memory, but it will also run on machines with shared memory architecture. One of the distinguishing features of PALM (missing from UCLALES) is that it contains modules to account for the surface topography, which allows the representation of surface obstacles such as buildings, hills or trees.

PALM was used in **Paper IV** to simulate the Puijo hill topography. Simulating the cloud microphysics with detailed surface representation is computationally heavy due to the high model resolution needed. Also, PALM lacks a detailed representation of aerosol cloud interactions. In **Paper IV,** an alternative computationally feasible approach was used to study cloud microphysics. Using the flow fields from PALM, particle trajectories were generated in order to study how the topography affects the vertical motion of air parcels. Those particle trajectories were later used as an input for a cloud parcel model to study the microphysics of aerosols and cloud droplets to see how the topography affects cloud droplet formation.

4.5. UCLALES-SALSA

In this thesis, SALSA is coupled to UCLALES with different levels of complexity. In the first implementation, only the standard version of SALSA was included. Aerosol mass and volume mixing ratios in different size bins are described as additional tracers in UCLALES. In the standard version of UCLALES (Stevens and Seifert, 2008), a warm-rain microphysical scheme (Seifert and Beheng, 2006) is implemented which uses a constant cloud droplet number concentration (CDNC). We modified this scheme by introducing CDNC as an advecting tracer, allowing CDNC to vary spatially and temporally (**Paper II**). The water supersaturation needed to calculate the aerosol activation was not available, because the saturation adjustment scheme is used to calculate the liquid water content. To calculate aerosol activation, we used our CPM (Kokkola et al., 2003a, 2003b) to generate a parameterization of the droplet concentration as a function of aerosol number concentration (pre-described size distribution), cooling rate and updraft velocity.

Another important new feature of the model is the implementation of a simple land surface model. In the default version of UCLALES, surface heat fluxes are prescribed (**Paper I**) but in UCLALES-SALSA (**Paper II** and **III**), heat fluxes were determined with the parameterization for soil energy balance, which was coupled with the radiation scheme (Ács et al., 1991). This allowed interactive simulations in case of radiation fogs.

UCLALES-SALSA was further used to implement a fully interacting sectional description of aerosols, clouds and precipitating particles in **Paper III**. Two methods are available for simulating the formation of cloud droplets in SALSA. One is the parameterization by Abdul-Razzak and Ghan (2002), which takes as an input the aerosol properties and updraft velocity (along with atmospheric thermodynamic properties) to determine the maximum supersaturation in a parcel of air and thus, the critical particle diameter for activation. Another is based on computing the supersaturation in each grid box and the explicit simulation of water condensation on particles. Once the wet diameter of a particle exceeds the critical diameter corresponding to the resolved supersaturation from the host model, the particle is activated as a cloud droplet. This parameterization is useful when the model vertical resolution is not enough to capture maximum supersaturation at the cloud phase.

5. Modelling application

5.1. Artificial injection of sea-salt particles in a marine environment

Following the idea of marine cloud brightening (MCB) (discussed in section 2.5) and the recommendations of Korhonen et al., (2010), we used UCLALES-SALSA to test the artificial injection of sea-salt particles in a marine environment at high resolution. After the work of Korhonen et al., (2010) both Wang et al., (2011) and Jenkins et al., (2013b) have employed cloud-resolving models to study how MCB works in realistic atmospheric conditions. In both of these studies, a relatively low resolution of 300 m was used, which is not enough to capture the particle loss rate near the emission source, where the particle concentration is highest. Stuart et al., (2013) used a very high resolution (0.5 m horizontally) to mimic the emission source in a LES model in order to observe particle loss through coagulation, and they observed particle losses of up to 50% in some specific conditions. With our model, we used an intermediate resolution (50 m) to resolve the small-scale turbulence and to capture the particle loss near the source point. We aimed to assess how well particles disperse in the boundary layer before they enter the cloud, and to estimate the particle loss rate through coagulation and sedimentation before they become cloud droplets. We also explicitly simulated the effect of water evaporating from (or condensing on) the sprayed sea-salt particles, a process which researchers have speculated to be important before, but which has only been approximated so far (Jenkins et al., 2013b).

Using a 50 m horizontal and 10 m vertical resolution in a domain size of 4.8 x 8.4 x 1.5 km, we introduced an emission source that moves perpendicular to the wind direction and emits sea-salt particles at a rate of 15 kgs^{-1}, with the salinity of sea water being 35 gkg^{-1}. Using this setup, we performed various simulations and found that at such a high resolution, the model is able to represent the emission source and dispersion of particles within the domain. The model also successfully captures the particle loss through coagulation, dry deposition, and the evaporation of water, the last of which leads to the occurrence of negative buoyancy and thus to increased particle loss.

With this setup, we performed a set of simulations where the relative importance of the considered microphysical processes was assessed by switching off different processes. We also performed the same set of simulations at different times of day and with different resolutions (**Paper I)**. The baseline simulation includes all of the microphysical processes, i.e. the water evaporation effect, coagulation, and sedimentation. The major findings from our simulation are:

1. We observed a delay in particle transport to the cloud layer and an increased particle loss as compared with the simulations in which aerosol water evaporation was not taken into account. This delay is mainly because of the evaporative cooling, which occurs when the emitted plume is mixed with the drier surroundings. Due to this cooling, relative humidity increases and buoyancy decreases. This effect is illustrated in Fig. 8.
2. The lifetime of the formed cold pool is short during the night. The results were much more striking when the simulations were repeated in the daytime (i.e. at 13:00) setup.

During the day, the mixing of the boundary layer is slower, which results in higher particle concentrations near the surface, and thus enhances the particle loss through coagulation and sedimentation.

3. In order to quantify the effect of water evaporation on particle transport and particle loss, we repeated the simulations with water evaporation switched off (illustrated by the blue plume in Fig. 8). We found that the delay in particle transport due to water evaporation amounts to about 10 min during the night and 20 min during the day. We found a maximum loss of 20% of all particles, which means that 80% of the particles remain in the air and are spread uniformly in the domain after 5 hours of emission.
4. The results in **Paper I** also highlight the importance of the model resolution used. With a resolution of 300 m, which was also used in Jenkins et al., (2013b), the maximum concentration of emitted particles was lower and the cold pool was not as cold as with the higher (50 m) resolution. The temperature decrease due to evaporation was only 0.4 K and thus the lifetime of the cold pool was much shorter and fewer particles were lost (3.1 %) through coagulation and deposition during the emission time.

The results of our study show that earlier global and cloud resolving model studies may have overestimated the effective CCN enhancement of MCB. However, this over-estimation is probably not enough to invalidate the findings. The scheme still holds the potential to counteract GHG-induced warming, but more detailed studies and experiments are needed to understand the effect of microphysical processes in order to ensure the efficacy of this technique. We do however suggest that, while designing the actual emission vessels or when performing further global scale modelling studies, the findings of high-resolution models should be taken into account.

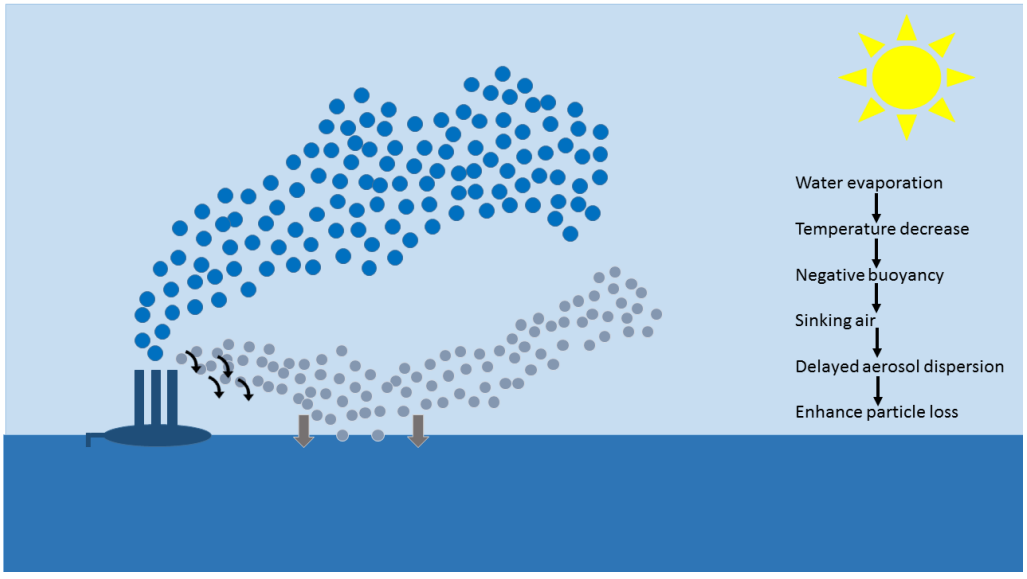

Figure 8: Schematic illustration showing the difference in artificial sea spray with (gray) and without (blue) water evaporation. Black arrows show the buoyancy effect near the emission source

5.2. Radiation fog

Compared with clouds, fogs are much less frequently studied with detailed models. As mentioned in Sec. 2.2, fog droplet properties are similar to those of cloud droplets, and aerosols can be expected to affect fog droplet concentrations. Also, the recent findings of the decreasing frequency of dense fog events with improving air quality support this hypothesis. However, as the cooling rate at the top of the fog is quite small, the situation is similar to clouds with low updraft velocities, and thus the fog droplet concentration should not be sensitive to the aerosol concentration (Reutter et al., 2009). Instead, radiation fog has been shown to be sensitive to meteorological conditions, surface properties and atmospheric radiation (Bott et al., 1990; Gultepe et al., 2007). In the scientific community, the relationship between aerosol concentration and radiation fog life cycle is still an open question. We used UCLALES-SALSA (**Paper II**) and UCLALES-CLOUD-SALSA (**Paper III**) to simulate radiation fog events in order to assess this relation.

With the first implementation of UCLALES-SALSA (**Paper II**), we used a parameterization for fog droplet activation, which was a function of the cooling rate. We assumed a log-normally distributed population of ammonium sulphate and black carbon (BC) particles as aerosol background. Ammonium sulphate acts as the cloud condensation nuclei (CCN) while BC, being a strong absorber of radiation, is assumed to counteract the CCN effect. We neglected aerosol sedimentation, coagulation, and all fog feedback to the aerosol for simplicity. Thus, aerosol-droplet interaction only accounted for droplet activation. These simplifications are justified, as the goal of Paper II was only to get an overall picture of the aerosol effect on radiation fog without comparison to any observations. With this model setup, we performed simulations to generate radiation fog using a resolution as high as 4 m in the horizontal and 1 m in the vertical direction. In the reference simulation, we neglected black carbon and introduced only ammonium sulphate with a mixing ratio of 800 #/mg and a log-normal aerosol size distribution with a geometrical mean diameter of 200 nm. The fog appeared during the night and grew vertically after formation. The parameterization for the droplet activation worked well: particles activated at the top of the fog, followed by growth and sedimentation down to the surface.

Our simulations revealed a positive feedback mechanism that made the fog more sensitive than expected to changes in aerosol loading. We observed a strong increase in radiative cooling at the top of the fog because of increases in aerosol loadings. This was caused by an originally small increase in water content due a larger number concentration of cloud droplets. Thus, the radiative cooling became stronger, enhancing the activation more than the increase of aerosol loading could have done. This positive feedback loop is substantial and we found it to be a major factor in radiation fog development. It is also important to note here that during the dissipation phase, when the fog detaches from the ground and transforms into a cloud, activation also happens at the base. From our simulation results, we conclude two main findings:

1. With increasing CCN concentration, the droplet concentration increases only slightly. However, even a small CDNC increase decreases the mean size of the droplets and

delays their sedimentation. Thus, LWC increases at the top of the fog, enhancing the radiative cooling, which feeds back into the number of formed droplets.

2. During sunny hours, the presence of absorbing aerosol (e.g. BC) counteracts fog development and speeds up fog dissipation. However, this BC warming effect is much smaller than the CCN effect on fog development.

The model setup used in **Paper II** had one severe shortcoming, as it was difficult to estimate the exact altitude where the droplets formed. The maximum cooling rate is not at the fog top, but slightly below it. However, it is not obvious that the maximum cooling rate is at the same altitude as the maximum supersaturation, but in our parameterization, particles were forced to activate at the same altitude as the fog top. With the new model setup of **Paper III**, this issue could be avoided, as particles are activated when they reach their critical size. In Fig. 9, we compare both models by using an initial CCN mixing ratio of 400 #/mg. Figure 10a shows the results using the parameterization of **Paper II**. Here, one can clearly see the strong activation at the top of the fog, and below it, the monotonously decreasing CDNC, which is due to droplet sedimentation and coagulation. The effective separation of the cooling rate and supersaturation in **Paper III** allows for droplet activation inside the fog, which happens after sunrise due to turbulent mixing. Figure 10 shows the relation between supersaturation (Fig. 10a) and cooling rate (Fig. 10b) for the model setup of **Paper III**. Simulating the radiation fog with UCLALES-CLOUD-SALSA reproduces the feedback loops we found in **Paper II**, which thus validates our earlier findings with UCALES-SALSA.

3. As higher aerosol loading leads to stronger radiative cooling at the top, the radiative cooling at the surface decreases. The warm surface creates an unstable temperature profile, which results in higher turbulent mixing near the surface. Thus, more droplets are formed at the fog base or within the fog during the dissipation phase.

Overall, our modelling results show that aerosols effectively affect the radiation fog's microphysical properties due to the above two positive feedback loops. Our results also are in line with the two phenomena observed in parallel, of a decrease in pollution and low visibility conditions.

UCLALES-CLOUD-SALSA was further used to simulate radiation fog events that took place at Cardington, UK in Feb. 2008 (Porson et al., 2011; Price, 2011). Our simulation results with zero wind profile agree with the campaign measurements. However, in this simulation we could not achieve a maximum fog height that was comparable to the measurements. We therefore performed an additional simulation where we introduced a wind profile, which resulted in an enhanced vertical development and also more droplet activation inside the fog. This happened because the introduced wind causes turbulence, which enhances the mixing and thus, amplifies the feedback loops.

Another important feature to note is that an increase in droplet concentration increases the liquid water path (LWP) and thus delays the warming and fog dissipation after sunrise. We expect that, because the surface warms less during a foggy day, a potential new fog will form earlier during the next evening/night. In order to simulate this behaviour, the role of the land-

atmosphere interaction is very important. We therefore suggest the implementation of a detailed land-surface model in order to simulate such cases.

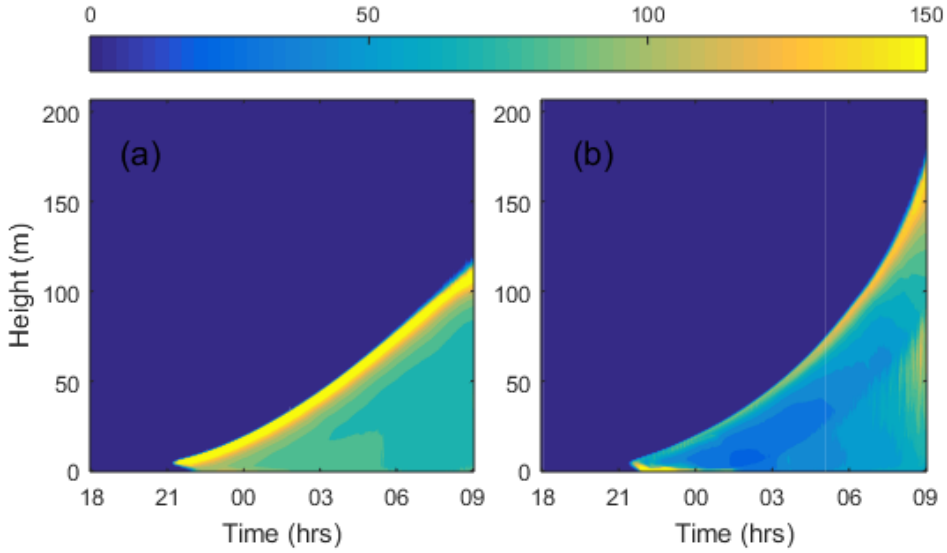

Figure 9: CDNC profile (#/mg) with an initial mixing ratio of 400 #/mg with (a) UCLALES-SALSA and with (b) UCLALES-CLOUD-SALSA.

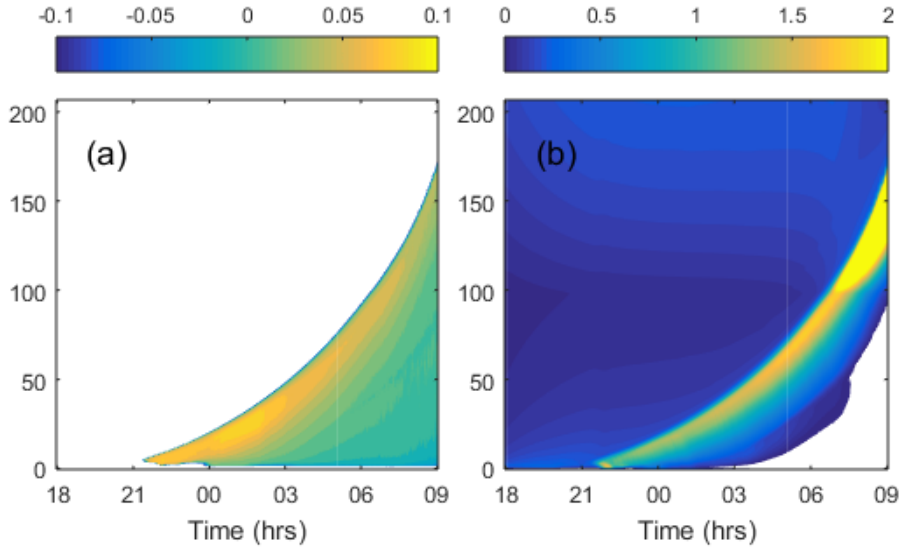

Figure 10: (a) shows the supersaturation profile of the simulations performed with UCLALES-CLOUD-SALSA using initial CCN 400 #/mg and (b) shows the cooling rate (Wm^{-2}) of the same simulation.

5.3. Cloud Droplet Activation

In clouds, most of the cloud droplets are activated at the cloud base, where the supersaturation is usually highest. At the cloud top, like in radiation fogs, droplet activation is mostly driven by radiative cooling, or by increased supersaturation due the mixing of air masses. Inside the cloud layers, additional droplet activation may occur due to turbulent mixing or local updrafts. We observed a similar phenomenon in our fog studies **(Paper III)**. Sloped or hilly areas provide good case studies to understand this phenomenon, because such slopes cause local updrafts. The observations (Hao et al., 2013, Portin et al., 2014, Väisänen et al., 2016) at Puijo hill measurement station as well as comparable studies elsewhere (Hammer et al., 2014, 2015) also indicate such in-cloud droplet activation. In **Paper IV**, we used Puijo measurement station observational data to model the effect of high updrafts caused by Puijo hill using the PALM large eddy model and our cloud parcel model.

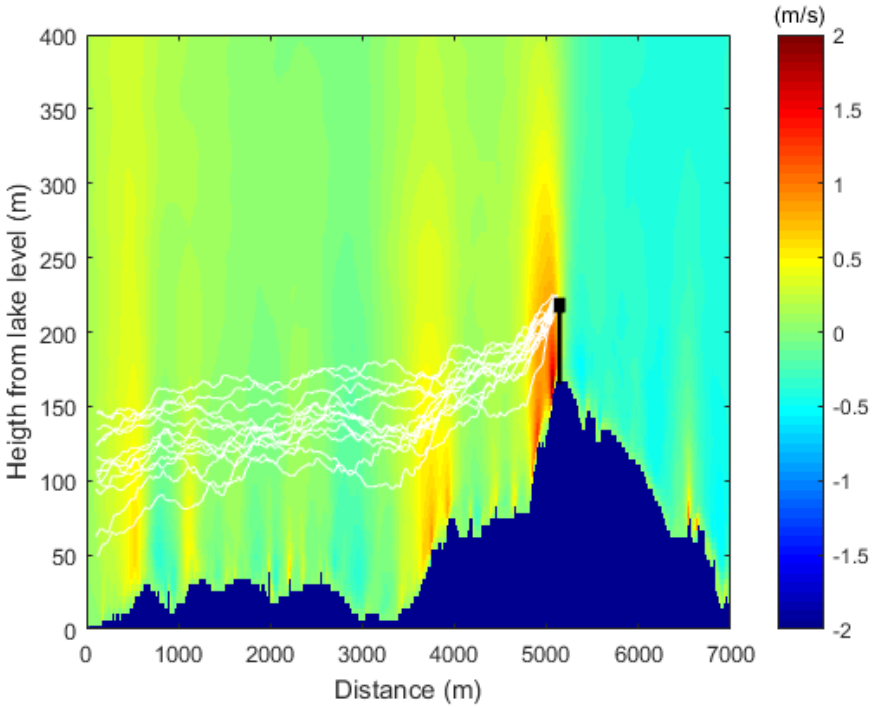

Figure 11: Simulated average wind fields and example trajectories of air parcels. In the topography plot, a forest height 17 m is assumed (Figure from **Paper IV)**.

The updraft is strongest near the surface and decreases as a function of height, which makes it difficult to assess its effect on cloud activation if the measurement station is located in a high tower. The topography-dependent flow fields around Puijo tower were modelled using the PALM large eddy model (Raasch and Schröter, 2001, Maronga et al., 2015). The flow trajectories obtained from the PALM were then used in our cloud parcel model (CPM) to study the cloud microphysics. Figure 11 shows the topography of the area and a few selected trajectories obtained from PALM. The CPM simulations show that the supersaturation at the cloud base is 0.2 %, while the updraft due to the hill causes supersaturation inside the cloud that can be as high as 0.4 %. If the in-cloud supersaturation becomes much higher than the

supersaturation at the cloud base, new droplets may form. However, for the accumulation mode particles, this secondary activation can cause only a limited increase in CDNC. The Aitken mode particles need much higher supersaturations to activate, because Aitken mode particles are smaller and usually also composed of lower hygroscopicity compounds. The second activation leads to a bimodal cloud droplet size distribution. Our results show that the newer and smaller droplets grow to around 5 – 7 μm and larger ones between 8 – 12 μm. These results agree well with the measurements at Puijo tower.

5.4. Aerosol and cloud dynamics

UCLALES has been used in the past to study boundary layer cloud dynamics (e.g. Stevens et al., 2005). The use of a high resolution enables LES models to represent the cloud structure and its dynamics in great detail (Ackerman et al., 2009). However, the detailed treatment of cloud and aerosol microphysics remains difficult because of the high computational burden. Therefore, the default version of UCLALES does not contain any description of aerosols, as is the case for most of the LES models. Instead, it assumes a prescribed cloud droplet concentration. Using the detailed aerosol description in UCLALES-CLOUD-SALSA, the aerosol cloud interactions, including cloud feedback to aerosol, can be studied in detail. In order to test the explicit representation of cloud droplets and precipitation, UCLALES-CLOUD-SALSA was configured with data from the DYCOMS-2 flight RF02 (Stevens et al., 2003). The model simulations were performed using the same setup used in Ackerman et al., (2009). In order to evaluate the aerosol effect, we also performed simulations with the default version of UCLALES, using the same setup.

In the simulations performed in **Paper III,** UCLALES-CLOUD-SALSA formed a stratocumulus cloud layer below the inversion layer. During the simulation, the cloud processing decreased the concentration of CCN, and together with sunrise and decreased radiative cooling, that led to the formation of precipitation. This was followed by the transition of the cloud state from stratocumulus to cumulus type clouds, resembling open cell circulation structures, a trend that was also observed during RF02 (Stevens et al., 2003). On the other hand, a thick cloud layer was produced and maintained in the simulations with default UCLALES.

During the day, the shortwave heating by the solar irradiation counter-acts the longwave radiative cooling at the cloud top and thus reduces the cloud driven mixing. This reduction in mixing supports the formation of a decoupled structure of the boundary layer. Efficient wet removal of the aerosols, which leads to a thinner cloud, makes this cloud-topped boundary layer even more sensitive to undergoing such changes. In this way, a feedback loop is formed, where wet removal reduces the aerosol concentration, which reduces droplet concentrations, and thus speeds up precipitation. This is similar to what has been observed in the transition from closed to open cellular structures in marine stratocumulus. However, the model domain used in our simulations was too small (5km x 5km) to notice such a change in mesoscale cloud organisation.

6. Conclusions

The response of cloud properties to changes in aerosols contributes one of the largest uncertainties to current projections of climate change. Aerosol-cloud interactions involve processes occurring at microscopic level. In this thesis, these processes are accounted for in lot of detail when aerosol-cloud interactions are studied at high resolution. The main focus was to develop, validate and refine the representation of aerosols and related processes in the large eddy model UCLALES. To this end, the sectional aerosol module SALSA was implemented in UCLALES, and SALSA was further modified to represent the cloud droplet size distribution and the precipitation droplets with a sectional size resolving method. In the different research questions studied, UCLALES-SALSA performed well in simulating the aerosol microphysics and cloud/fog dynamics, fulfilling the first objective set for the thesis.

The second objective was to study the role of explicit aerosol microphysics on the efficacy of marine cloud brightening, especially to account for water evaporation from sprayed sea water (**Paper I**). The inclusion of SALSA in UCLALES and detailed implementation of microphysical processes related to condensation and coagulation proved essential for addressing the behaviour of the particles after emission. The model realistically captures the buoyancy effect due to water evaporation, which ultimately leads to a higher particle loss rate due to sedimentation and coagulation processes, and a delay in particle mixing in the ABL. The overall results of the sea spray simulations (**Paper I**) show that the geo-engineering method of marine cloud brightening (MCB) could have the potential to counteract global warming, but more high-resolution studies are needed to quantify the overall efficacy of this method.

Like in clouds, aerosols affect the fog life cycle, and testing this was set as a third objective. UCLAES-SALSA was used to simulate radiation fogs and the fog behaviour was analysed under different aerosol loadings. With the original version of SALSA, the model simulates the activation of fog droplets by using a parameterization that depends on the aerosol number concentration, updraft velocity, and cooling rate. The modelling results show that the fog life cycle is sensitive to the concentration of both CCN and absorbing aerosol, but the CCN effect dominates (**Paper II**). The findings from Paper II were partly revisited in Paper III, where the full UCLALES-SALSA was employed and thus, droplet activation was calculated explicitly. We observed two important positive feedback loops connected to aerosol-fog interaction (**Paper II** and **III**). First, a higher aerosol loading leads to smaller droplets, which slows the droplet sedimentation. This delay in sedimentation increases the liquid water content, which enhances the radiative cooling at the fog top, which, in turn, leads to more efficient droplet formation. Second, the increase in radiative cooling at the top of the fog weakens the cooling of the surface, which leads to the formation of turbulence near the surface. This facilitates particle activation inside the fog layer before and during the dissipation phase. The existence of these feedback loops supports the hypothesis that the decreasing frequency of fog events all over Europe is connected to the decreasing trends in aerosol concentrations.

The last objective was to study how aerosol particles activate into cloud droplets. The importance of droplet formation in different aspects of radiation fog development was already shown in papers II and III. In addition, in the case of boundary layer clouds, the strong updrafts

due to surface topography (hills, slopes etc.) also affect the cloud droplet activation. Puijo hill, located in Kuopio (Finland), provided a useful case study to analyse the effect of updraft on cloud droplet activation. The results show that high supersaturation can occur inside the cloud, leading to a bi-modal cloud droplet size distribution. This was both modelled as well as observed at the Puijo station. However, in-cloud supersaturation causes only limited enhancement in the cloud droplet number concentration (CDNC).

There is a great demand for more accurate and reliable high resolution models for a variety of applications. This includes higher resolution climate simulations, predictions, re-analysis and comparison with observations. Significant advances beyond the current state-of-the-art climate modelling capability are needed in order to overcome the current limitations. In view of recent progress in computer resources, high-resolution models are now in the spotlight. LES models, with their ability to resolve large energy containing eddies, are proving to be a useful tool for understanding the complex microphysical processes that occur at resolutions of down to a few metres. In the context of climate change, the understanding of ACI is still poor. In order to generate reliable future climate projections, the understanding of ACI is vital. This thesis is an attempt to highlight that high resolution LES models are a useful tool for understanding ACI. The uncertainties associated with ACI can be addressed with such tools.

7. Review of the papers and the author's contribution

Paper I investigates the efficacy of artificial sea-salt geoengineering in the marine environment, especially how the interaction between sprayed sea water and the environment affects the dispersion of the particles. When sea spray is released to ambient RH lower than the water saturation over the seawater particle, the evaporating water decreases the ambient temperature and thus causes negative buoyancy, which could result in delaying the transport of particles to the top of the boundary layer. Additionally, we also studied the number loss of the aerosol particles through coagulation and dry deposition on the surface near the source point before being mixed over the boundary layer. The effect of model resolution in studying aerosol processes was also discussed. I was the main developer of the early version of UCALES-SALSA used in **paper I,** and performed all the simulations. I also wrote the paper and did all of the data analysis together with the co-authors.

Paper II studies how aerosol affects the properties and lifecycle of radiation fog. It showed that the changes in CCN concentration produce feedback mechanisms that makes radiation fog highly susceptible to changes in aerosol properties, thus supporting the observations of the decreasing frequency of low visibility events with improving air quality. The paper also shows that BC, as an absorbing aerosol, has a noticeable effect on fog height and dissipation time but its relative effect compared to changes in the CCN concentration is small, even if BC concentration is high. The sensitivity of fog formation to meteorological conditions was also discussed. For the paper, I performed all the simulations, participated in the results analysis and wrote the paper together with the co-authors. The aerosol-radiation interaction code used was developed and implemented by Dr Thomas Kühn.

Paper III contains the description and evaluation of the fully coupled UCLALES-SALSA model. The new model is based on the UCLALES model, coupled with an extended version of the SALSA, which contains sectional descriptions for aerosols, clouds and precipitating particles. The strategy for the layout of the cloud droplet bins emphasises the tracking of size-resolved aerosol particle properties both in- and outside of clouds and through cloud cycles. As an example case of the model's skill at representing aerosol-cloud interactions, the simulation results for marine stratocumulus clouds and radiation fogs were presented. For the paper, I participated in the model development, which was mainly carried out by Dr Juha Tonttila. I performed fog simulations, and participated in the results analysis and commented on the manuscript.

Paper IV reports the effect of surface topology on the cloud droplet formation in the case of low level stratus clouds. The topology around the Puijo hill measurement station was included in the PALM large eddy model simulator to simulate the 3D winds arriving at the station. A set of trajectories was obtained from the simulations, and used as an input for the cloud parcel

model, to study aerosol-cloud droplet microphysics in detail. As a result, it was shown that the hill might induce updrafts that are strong enough to cause cloud droplet formation inside the cloud as well as at the bottom. This was seen both in the measurement data and the modelling results. I performed the cloud parcel model simulations, and analysed the results related to cloud droplet size distributions from both the simulations and the measurements. I also contributed to the finalisation of the manuscript.

References

Abdul-Razzak, H. and Ghan, S. (2002). A parameterisation of aerosol activation 3. Sectional representation. *J. Geophys. Res.*, 107(D3).

Ackerman, A.S., vanZanten, M.C., Stevens, B., Savic-Jovic, V., Bretherton, C.S., Chlond, A., Golaz, J-C., Jiang, H., Khairoutdinov, M., Krueger, S.K., Lewellen, D.C., Lock, A., Moeng, C-H., Nakamura, K., Petters, M.D., Snider, J.R., Weinbrecht, S., and Zulauf, M. (2009). Large-eddy simulations of a drizzling, stratocumulus-topped marine boundary layer. *Mon. Weather Rev.*, 137, 1083–1110.

Albrecht, B. (1989). Aerosols, Cloud Microphysics, and Fractional Cloudiness. *Science*, 245, 1227–1230.

Almeida, J., Schobesberger, S., Kürten, A., Ortega, I. K., Kupiainen-Määttä, O., Praplan, A. P., Adamov, A., Amorim, A., Bianchi, F., Breitenlechner, M., David, A., Dommen, J., Donaue, N. M., Downard, A., Dunne, E., Duplissy, J., Ehrnhart, S., Flagan, R. C., Franchin, A., Guida, R., Hakala, J., Hansel, A., Heinritzi, M., Henschel, H., Jokinen, T., Junninen, H., Kajos, M., Kangasluoma, J., Keskinen, H., Kupc, A., Kurtén, T., Kvashin, A. N., Laaksonen, A., Lehtipalo, K., Leiminger, M., Leppä, J., Loukonen, V., Makhmutov, V., Mathot, S., McGrath, M. J., Nieminen, T., Olenius, T., Onnela, A., Petäjä, T., Riccobono, F., Riipinen, I., Rissanen, M., Rondo, L., Ruuskanen, T., Santos, F. D., Sarnela, N., Schallhart, S., Schnitzhofer, R., Seinfeld, J. H., Simon, M., Sipilä, M., Stozhkov, Y., Stratmann, F., Tom_e, A., Tröstl, J., Tsagkogeorgas, G., Vaattovaara, P., Viisanen, Y., Virtanen, A., Vrtala, A., Wagner, P. E., Weingartner, E., Wex, H., Williamson, C., Wimmer, D., Ye, P., Yli-Juuti, T., Carslaw, K. S., Kulmala, M., Curtius, J., Baltensperger, U., Worsnop, D. R., Vehkamäki, H., and Kirkby, J. (2013). Molecular understanding of sulphuric acid-amine particle nucleation in the atmosphere. Nature, 502:359-363.

Alterskjær, K., and Kristjánsson J. E. (2013). The sign of the radiative forcing from marine cloud brightening depends on both particle size and emission amount. *Geophys. Res. Lett.*, 40,210–215.

Alterskjaer, K., Kristjansson, J. E., Boucher, O., Muri, H., Niemeier, U., Schmidt, H., Schulz, and M., Timmreck, C. (2013). Sea-salt injections into the low-latitude marine boundary layer: The transient response in three Earth system models. *J. Geophys. Res. Atmos.*, 118, 12,195–12,206.

Andrejczuk, M., Grabowski, W.W., Malinowski, S.P., Smolarkiewicz, P.K. (2006). Numerical simulation of cloud-clear air interfacial mixing: effects on cloud microphysics. J Atmos Sci., 63:3204–25.

Applegate, P.J., and Keller, K. (2015). How effective is albedo modification (solar radiation management geoengineering) in preventing sea-level rise from the Greenland Ice Sheet? *Environmental Research Letters.*, 10:084018.

Argyropoulos, C., and Markatos, N. (2015). Recent advances on numerical modelling of turbulent flows. *Appl. Math. Model.* 39 (2) 693e732.

Ács, R., Mihailocic, D.T., and Rajkovic, B. 1991. A coupled soil moisture and surface temperature prediction model. J. Appl. Meteorol. 30, 812e822.

Beare, R.J., MacVean, M.K., Holtslag, A.A.M., Cuxart, J., Esau, I., Golaz, J-C., Jimenez, M. A., Khairoutdinov, M., Kosovic, B., Lewellen, D., Lund, T.S., Lundquist, J.K., McCabe, A., Moene, A.F., Noh, Y., Raasch, S., and Sullivan, (2006). An Intercomparison of Large-Eddy Simulations of the Stable Boundary Layer. *Boundary-Layer Meteorol.*, 118: 247-272.

Bond, T.C., Doherty, S.J., Fahey, D.W., Forster, P.M., Berntsen, T., DeAngelo, B.J., Flanner, M.G., Ghan, S., Kärcher, B., Koch, D., Kinne, S., Kondo, Y., Quinn, P.K., Sarofim, M.C., Schultz, M.G., Schulz, M., Venkataraman, C., Zhang, H., Zhang, S., Bellouin, N., Guttikunda, S.K., Hopke, P.K., Jacobson, M.Z., Kaiser, J.W., Klimont, Z., Lohmann, U., Schwarz, J.P., Shindell, D., Storelvmo, T., Warren, S.G., and Zender, C.S.: Bounding the role of black carbon in the climate system: A scientific assessment, *J. Geophys. Res.*, 118, 5380–5552.

Bony, S., Stevens, B., Frierson, D.M.W., Jakob, C., Kageyama, M., Pincus, R., Shepherd, T.G., Sherwood, S.C., Siebesma, A.P., Sobel, A.H., Watanabe, M., Webb, M.J. (2015). Clouds, circulation and climate sensitivity. *Nat Geosci.*, 8:261–268.

Bott, A., (1991). On the influence of the physico-chemical properties of aerosols on the life cycle of radiation fogs. *Boundary-Layer Meteorol*. 56, 1–31.

Boucher, O., Randall, D., Artaxo, P., Bretherton, C., Feingold, G. et al.: Clouds and aerosols. In: Stocker, T.F., Qin, D., Plattner, G.-K., Tignor, M., Allen, S. K., Boschung, J., Nauels, A., Xia, Y., Bex, V., Midgley, P. M. (Eds.): Climate change (2013). The physical science basis. Contribution of Working Group I to the Fifth Assessment Report of the Intergovernmental Panel on Climate Change. Cambridge: University Press 2013.

Bower, K., Choularton, T., Latham, J., Sahraei, J., and Salter S. (2006). Computational assessment of a proposed technique for global warming mitigation via albedo-enhancement of marine stratocumulus clouds. *Atmos. Res.* ,82, 328–336.

Brown A.R., Cederwall R.T., Chlond A., Duynkerke P., Golaz J.-C., Khairoutdinov M., Lewellen D.C., Lock A.P., MacVean M.K., Moeng C.-H., Neggers R.A.J., Siebesma A.P. and Stevens B. (2002). Large-eddy simulation of the diurnal cycle of shallow cumulus convection over land. *Quart. J. Roy. Meteor. Soc.,* 128, 1779–1798.

Chang, D., Song, Y., and Liu, B. (2009). Visibility trends in six megacities in China 1973–2007. *Atmos. Res.,* 94, 161–167.

Clarke, A., Kapustin, V., Howell, S., Moore, K., Lienert, B., Masonis, S., Anderson, T., and Covert, D. (2003). Sea-salt size distributions from breaking waves: Implications for marine aerosol production and optical extinction measurements during SEAS. *J. Atmos. Oceanic Technol.,* 20, 1362–1374.

Croft, B., Lohmann, U., Martin, R.V., Stier, P., Wurzler, S., Feichter, J., Hoose, C., Heikkilä, U., van Donkelaar, A., and Ferrachat, S. (2010). Influences of in-cloud aerosol scavenging parameterizations on aerosol concentrations and wet deposition in ECHAM5-HAM. *Atmos. Chem. Phys.,* 10, 1511–1543.

DeMott, C. A., Stan, C., Randall, D. A., Kinter J. L. III, and Khairoutdinov, M. (2011). The Asian Monsoon in the super-parameterized CCSM and its relation to tropical wave activity. *J. Clim.,* 24, 5134–5156.

Diner, D., Ackermann, T.P., Anderson, T.L., Bosenberg, J., Braverman, A., Charlson, R., et al. (2004). PARAGON: an integrated approach for characterising aerosol climate impacts and environmental interactions. *BAMS.,* 85:1491 – 501.

Ehn, M., Thornton, J. A., Kleist, E., Sipila, M., Junninen, H., Pullinen, I., Springer, M., Rubach, F., Tillmann, R., Lee, B., Lopez-Hilfiker, F., Andres, S., Acir, I.-H., Rissanen, M., Jokinen, T., Schobesberger, S., Kangasluoma, J., Kontkanen, J., Nieminen, T., Kurten, T., Nielsen, L. B., Jorgensen, S., Kjaergaard, H. G., Canagaratna, M., Maso, M. D., Berndt, T., Petaja, T., Wahner, A., Kerminen, V.-M., Kulmala, M., Worsnop, D. R., Wildt, J., and Mentel, T. F. (2014) A large source of low-volatility secondary organic aerosol, *Nature.,* 506, 476–479.

Feng, J. (2007). A 3-mode parameterization of below-cloud scavenging of aerosols for use in atmospheric dispersion models. *Atmos. Environ.,* 41, 6808–6822.

Forster, P., Ramaswamy, V., Artaxo, P., Berntsen, T., Betts, R., Fahey, D.W., Haywood, J., Lean, J., Lowe, D.C., Myhre, G., Nganga, J., Prinn, R., Raga, G., Schulz, M., and Van Dorland, R. (2007). Climate Change 2007, The Physical Science Basis, Contribution of Working Group I to the Fourth Assessment Report of the Intergovernmental Panel on Climate Change. Cambridge Univ. Press, Cambridge, United Kingdom, and New York, NY, USA.

Fu, Q. and Liou, K. N. (1993). Parameterization of the radiative properties of cirrus clouds. *J. Atmos. Sci.*, 50, 2008–2025.

Fuch, N.A., (1964). Mechanics of Aerosol. *Pergamon,* New York.

Fureby, C. (2008). Towards the use of large eddy simulation in engineering. *Prog. Aerosp. Sci.*, 44, 381–396.

Grabowski, W. W., and Smolarkiewicz, P. K. (1999). CRCP: A Cloud Resolving Convection Parameterization for modeling the tropical convecting atmosphere. *Physica D*, 133, 171–178.

Giulianelli, L., Gilardoni, S., Tarozzi, L., Rinaldi, M., Decesari, S., Carbone, C., Facchini, M.C., and Fuzzi, S. (2014). Fog occurrence and chemical composition in the Po valley over the last twenty years. *Atmospheric environment*., 98 394-401.

Gultepe, I., Tardif, R., Michaelides, S., Cermak, J., Bott, A., Bendix, J.,Muller, M.D., Pagowski, M., Hansen, B., Ellrod, G., Jacobs, W., Toth, G., and Cober, S.G. (2007). Fog research: a review of past achievements and future perspectives. *Pure Appl Geophys.*, 164, 1121–1159.

Hammer, E., Bukowiecki, N., Gysel, M., Jurányi, Z., Hoyle, C. R., Vogt, R., Baltensperger, U., and Weingartner, E. (2014). Investigation of the effective peak supersaturation for liquid-phase clouds at the high-alpine site Jungfraujoch, Switzerland (3580ma.s.l.). *Atmos. Chem. Phys.*, 14, 1123–1139.

Hammer, E., Bukowiecki, N., Luo, B.P., Lohmann, U., Marcolli, C., Weingartner, E., Baltensperger, U. and Hoyle, C.R. (2015). Sensitivity Estimations for Cloud Droplet Formation

in the Vicinity of the High Alpine Research Station Jungfraujoch (3580 m a.s.l.). *Atmos. Chem. Phys.*, 15: 10309–10323.

Hao, L.Q., Romakkaniemi, S., Kortelainen, A., Jaatinen, A., Portin, H., Miettinen, P., Komppula, M., Leskinen, A., Virtanen, A., Smith, J.N., Worsnop, D.R., Lehtinen, K.E.J., and Laaksonen A., (2013). Aerosol Chemical Composition in Cloud Events by High Resolution Time-of-Flight Aerosol Mass Spectrometry, *Environ. Sci. Technol.*, 47, 2645–2653.

Haywood, J. M., Donner, L. J., Jones, A., and Golaz, J.-C. (2009). Global indirect radiative forcing caused by aerosols: IPCC (2007) and beyond, in Clouds in the Perturbed Climate System, edited by J. Heintzenberg and R. J. Charlson. *MIT Press, Cambridge.*, pp. 451–467.

Heintzenberg, J., Graf, H.-F., Charlson, R.J., and Warneck, P. (1996). Climate forcing and the physico-chemical life cycle of the 25 atmospheric aerosol - Why do we need an integrated, interdisciplinary global research programme? *Contrib. Atmos. Phys.*, 69, 261–272.

Herzegh, P. H., Bankert, R. L., Hansen, B. K., Tryhane, M., and Wiener, G. (2004). Recent progress in the development of automated analysis and forecast products for ceiling and visibility conditions. Preprints, 20th Conf. on Interactive Information Processing Systems for Meteorology, oceanography, and Hydrology, Seattle, WA, Amer. *Meteor. Soc.*, CD-ROM, 3.3.

Hewitt, C. N., and Jackson, A. V. (2009) Atmospheric science for environmental scientists, Wiley.

Hinds, W.C. (1999) Aerosol Technology: Properties, behavior and measurements of airborne particles, Wiley, NY.

Holland, M., Hunt, A., Hurley, F., Navrud, S., Watkiss, P. (2005). Methodology for the cost–benefit analysis for CAFE: Volume 1: overviewof methodology. Service Contract for Carrying out Cost Benefit Analysis of Air Quality Related Issues, in particular in the Clean Air for Europe (CAFE) Programme. Didcot UK: AEA Technology Environment.

Holtslag, A.A.M., (2006). GEWEX atmospheric boundary-layer study (GABLS) on stable boundary layers. *Boundary-Layer Meteorology*., 118 (2), 243–246.

IPCC. Climate change 2013: The physical science basis. Contribution of the Working Group I to the Fifth Assessment Report of The Intergovernmental Panel on Climate Change. Cambridge University Press, Cambridge, United Kingdom and New York, NY, USA.

Irvine, P. J., Schäfer, S., Lawrence, M. G. (2014). Solar radiation management could be a game changer, *Nature, Clim. Change.*, 4(10), 842–842.

Irvine, P.J., Kravitz, B., Lawrence, M.G., Muri, H. (2016). An overview of the earth system science of solar geoengineering. *WIREs Clim Change*. 7:815–833.

Jacobson, M. Z. 2005. Fundamentals of atmospheric modeling. Cambridge University press, New York, 2nd edition.

Jacobson, M. Z. 2014. Effects of biomass burning on climate, accounting for heat and moisture fluxes, black and brown carbon, and cloud absorption effects. *J. Geophys. Res. Atmos*. 119(14): 2014JD021861.

Jenkins, A. K. L., Forster, P. M., and Jackson, L.S. (2013). The effects of timing and rate of marine cloud brightening aerosol injection on albedo changes during the diurnal cycle of marine stratocumulus clouds. *Atmos. Chem. Phys.*, 13, 1659–1673.

Jenkins, A. K. L., and Forster, P. M. (2013). The inclusion of water with the injected aerosols reduces the simulated effectiveness of marine cloud brightening. *Atmos. Science Letters* 14, 164–169.

Jensen, J., and Lee, S. (2008). Giant sea-salt aerosols and warm rain formation in marine stratocumulus, *J. Atmos. Sci.*, 65(12), 3678–3694.

Jones, A., Haywood, J. M. (2012), Sea-spray geo-engineering in the HadGEM2-ES earth-system model: radiative impact and climate response. *Atmos. Chem. Phys.*, 12, 10887–10898.

Järvinen, E., Virkkula, A., Nieminen, T., Aalto, P.P., Asmi, E., Lanconelli, C., Busetto, M., Lupi, A., Schioppo, R., Vitale, V., Mazzola, M., Petäjä, T., Kerminen, V.-M., and Kulmala, M. (2013). Seasonal cycle and modal structure of particle number size distribution at Dome C, Antarctica. *Atmos. Chem. Phys.*, 13, 7473–7487.

Kirkby, J., Curtius, J., Almeida, J., Dunne, E., Duplissy, J., Ehrhart, S., Franchin, A., Gagné, S., Ickes, L., Kürten, A., Kupc, A., Metzger, A., Riccobono, F., Rondo, L., Schobesberger, S., Tsagkogeorgas, G., Wimmer, D., Amorim, A., Bianchi, F., Bretenlechner, M., David, A., Dommen, J., Downard, A., Ehn, M., Flagan, R., Haider, S., Hansel, A., Hauser, D., Jud, W., Junninen, H., Kreissl, F., Kvashin, A., Laaksonen, A., Lehtipalo, K., Lima, J., Lovejoy, E., Makhmutov, V., Mathot, S., Mikkilä, J., Minginette, P., Mogo, S., Nieminen, T., Onnela, A., Pereira, P., Petäjä, T., Schnitzhofer, R., Seinfeld,J. H., Sipilä, M., Stozhkov, Y., Stratmann, F., Tom_e, A., Vanhanen, J., Viisanen, Y., Vrtala, A., Wagner, P. E., Walther, H., Weingartner, E., Wex, H., Winkler, P. M., Carslaw, K. S., Worsnop, D. R., Baltensperger, U., and Kulmala, M. (2011). Role of sulphuric acid, ammonia and galactic cosmic rays in atmospheric aerosol nucleation. Nature 476:429-433.

Kerminen, V.-M., Paramonov, M., Anttila, T., Riipinen, I., Fountoukis, C., Korhonen, H., Asmi, E., Laakso, L., Lihavainen, H., Swietlicki, E., Svenningsson, B., Asmi, A., Pandis, S. N., Kulmala, M., and Petäjä, T. (2012). Cloud condensation nuclei production associated with atmospheric nucleation: a synthesis based on existing literature and new results. Atmos. Chem. Phys., 12:12037-12059.

Korhonen, H., Carslaw, K.S., and Romakkaniemi, S. (2010). Enhancement of marine cloud albedo via controlled sea spray injections: a global model study of the influence of emission rates, microphysics and transport. *Atmos. Chem. Phys.,* 10, 4133–4143.

Kokkola, H., Romakkaniemi, S., and Laaksonen, A. (2003a). A one dimensional cloud model including trace gas condensation and sulfate chemistry. *Boreal Env. Res.*, 8: 413-424.

Kokkola, H., Romakkaniemi, S., and Laaksonen, A. (2003b). Köhler theory for a polydisperse droplet population in the presence of a soluble trace gas, and an application to stratospheric sts droplet growth. *Atmos. Chem. Phys.,* 3, 2139-2146.

Kokkola, H., Korhonen, H., Lehtinen, K.E.J., Makkonen, R., Asmi, A., Järvenoja, S., Anttila, T., Partanen, A.-I., Kulmala, M., Järvinen, H., Laaksonen, A., and Kerminen, V.-M. (2008). SALSA– a Sectional Aerosol module for Large Scale Applications. Atmos. *Chem. Phys.,* 8, 2469–2483.

Kulmala, M., Petäjä, T., Ehn, M., Thornton, J., Sipilä, M., Worsnop, D. R., and Kerminen, V.-M. (2014). Chemistry of Atmospheric Nucleation: On the Recent Advances on Precursor Characterization and Atmospheric Cluster Composition in Connection with Atmospheric New Particle Formation. Annu. Rev. Phys. Chem., 65:21-37.

Kühn, T., A. I. Partanen, A. Laakso, and Z. Lu, (2014). Climate impacts of changing aerosol emissions since 1996. *Geophys. Res. Lett.,* 41,4711–4718.

Laakso, A., Kokkola, H., Partanen, A.-I., Niemeier, U., Timmreck, C., Lehtinen, K. E. J., Hakkarainen, H., and Korhonen, H. (2016). Radiative and climate impacts of a large volcanic eruption during stratospheric sulfur geoengineering. *Atmos. Chem. Phys.,* 16, 305–323.

Latham, J. (1990). Control of global warming? *Nature.,* 347, 339–340.

Latham, J., Bower, K., Choularton, T., Coe, H., Connoly, P., Cooper, G., Craft, T., Foster, J., Gadian, A., Galbraith, L., Iacovides, H., Johnston, D., Launder, B., Leslie, B., Meyer, J., Neukermans, A., Ormond, B., Parkes, B., Rasch, P., Rush, J., Salter, S., Stevenson, T., Wang, H.,Wang, Q., and Wood, R. (2012). Marine cloud brightening. *Phil. Trans. Royal Society A.*, 370, 4217–4262.

Latham, J. Rasch, P. Chen, C-C. Kettles, L. Gadian, A. Gettelman, A. Morrison, H. Bower, K. and Choularton, T. (2008). Global temperature stabilization via controlled albedo enhancement of low-level maritime clouds. *Phil Trans Royal Society A.*, 366, 3969–3987.

Law, K. S., and Stohl, A. (2007). Arctic air pollution: Origins and impacts, Science, 315, 1537–1540.

Lohmann, U., and Feichter, J. (2005). Global Indirect aerosol effect: a review. *Atmos. Chem. Phys.,* 5, 715–737, 2005.

Lu, Z., Zhang Q., and Streets, D. G., (2011). Sulfur dioxide and primary carbonaceous aerosol emissions in China and India, 1996–2010. *Atmos. Chem. Phys.,* 11, 9839–9864.

Maronga, B., Moene, A. F., van Dinther, D., Raasch, S., Bosveld F., and Gioli, B. (2013). Derivation of structure parametres of temperature and humidity in the convective boundary layer from large-eddy simulations and implications for the interpretation of scintillometre observations. Boundary-Layer Meteorol., 148, 1-30.

Maronga, B., Gryschka, M., Heinze, R., Hoffmann, F., Kanani-Sühring, F., Keck, M., Ketelsen, K., Letzel, M. O., Sühring, M., and Raasch, S. (2015). The Parallelized Large-Eddy Simulation Model (PALM) version 4.0 for atmospheric and oceanic flows: model formulation, recent developments, and future perspectives. *Geosci. Model Dev.*, 8, 1539-1637.

McFiggans, G., Artaxo, P., Baltensperger, U., Coe, H., Facchini, M.C., Feingold, G., Fuzzi, S., Gysel, M., Laaksonen, A., Lohmann, U., Mentel, T.F., Murphy, D.., O'Dowd, C.D., Snider, J.R., and Weingartner, E. (2006). The effect of physical and chemical aerosol properties on warm cloud droplet activation. *Atmos. Chem. Phys.,* 6, 2593–2649.

Moeng, C.-H., Cotton, W.R., Bretherton, C., Chlond, A., Khairoutdinov, M., Krueger, S., Lewellen, W.S., MacVean, M.K., Pasquier, J.R.M., Rand, H.A., Siebesma, A.P., Stevens, B., Sykes, R.I. (1996). Simulation of a stratocumulus-topped planetary boundary layer: Intercomparison among different numerical codes. *American Meteorological Society,* 77. 2 261-278.

Myhre, G., Myhre, C.E.L., Samset, B.H., and Storelvmo, T. (2013). Aerosols and their relation to global climate and climate sensitivity, *Nature Education Knowledge,* 4(5):7.

Mönkkönen, P., Koponen, I.K., Lehtinen, K.E.J., Hameri, K., Uma, R., and Kulmala, M. (2005). Measurements in a highly polluted Asian mega city: Observations of aerosol number size distributions, modal parameters and nucleation events. *Atmos. Chem. Phys.,* 5, 57–66.

Nakanishi, M., (2000). Large-eddy simulation of radiation fog. *Boundary-Layer Meteorol.,* 94, 461–493.

Nenes, A., and Seinfeld, J. H. (2003). Parameterization of cloud droplet formation in global climate models. *J. Geophys. Res.,* 108(D14), 4415.

Park, S., Baik, J., Han, B. (2013). Large-eddy simulation of turbulent flow in a densely built-up urban area. Environ Fluid Mech., 1–16.

Partanen, A. I., Kokkola, H., Romakkaniemi, S., Kerminen, V. M., Lehtinen, K. E. J., Bergman, T., Arola, A., and Korhonen, H. (2012). Direct and indirect effects of sea spray geoengineering and the role of injected particle size. *J. Geophys. Res.,* 117, D02203.

Penner, J.E., Charlson, R.J., Hales, J.M., Laulainen, N., Leifer, R., Novakov, R., Ogren, J., Radke, L.F., Schwartz, S.E., Travis, L. (1994). Quantifying and minimizing uncertainty of climate forcing by anthropogenic aerosols. *Meteorol. Soc.,* 75, 375–400.

Petters, M. D. and Kreidenweis, S. M. (2007). A single parametre representation of hygroscopic growth and cloud condensation nucleus activity, Atmos. Chem. Phys., 7, 1961–1971.

Pierce, J.R., and Adams, P.J. (2007). Efficiency of cloud condensation nuclei formation from ultrafine particles. *Atmos. Chem. Phys.,* 7: 1367–1379.

Pincus, R., and Stevens, B. (2009). Monte Carlo spectral integration: A consistent appr oximation for radiative transfer in large eddy simulations. *J. Adv. Model. Earth Syst.,* 1-9.

Pincus, R., and Stevens, B. (2013). Paths to accuracy for radiation parameterizations in atmospheric models. *J. Adv. Model. Earth Syst.,* 5, 225–233.

Porson, A., Price, J., Luck, A., and Clark, P. (2011). Radiation fog. Part II: large eddy simulations in very stable conditions. *Boundary-Layer Meteorol.,* 139,193–224.

Portin, H., Leskinen, A., Kortelainen, A., Hao, L., Miettinen, P., Jaatinen, A., Lihavainen, H., Laaksonen, A., Lehtinen, K.E.J., Romakkaniemi, S., and Komppula, M. (2014). The effect of local sources on particle size and chemical composition and their role in aerosol–cloud interactions at Puijo measurement station. *Atmos. Chem. Phys.*, 14, 6021-6034.

Price, J., 2011. Radiation fog. Part I: observations of stability and drop size distributions.

Boundary-Layer Meteorology., 139, 167e191.

Pritchard, M. S., and Somerville, R. C. J. (2010). Assessing the diurnal cycle of precipitation in a multi-scale climate model. *J. Adv. Model. Earth Syst.,* 1-12.

Pruppacher, H.R., and Klett, J.D. (1978). Microphysics of Clouds and Precipitation. Reidel, Hingham, Massachusetts.

Putman, W. M., and Suarez, M. (2011). Cloud-system resolving simulations with the NASA Goddard Earth Observing System global atmospheric model (GEOS-5). *Geophys. Res. Lett.,* 38, L16809.

Raasch, S., and Schröter, M. (2001). PALM - a large-eddy simulation model performing on massively parallel computers. *Meteorol. Z.*, 10, 363–372.

Ramanathan, V., Carmichael, G. (2008). Global and regional climate changes due to black carbon. *Nat Geosci.*, 1:221–7.

Ramanathan, V. and Feng, Y. (2009). Air pollution, greenhouse gases and climate change: global and regional perspectives. *Atmos. Environ.*, 43, 37–50.

Randall, D., Khairoutdinov, M., Arakawa, A., and Grabowski, W. 2003. Breaking the cloud parameterization deadlock. Bull. *Am. Meteor. Soc.*, 84, 1547–1564.

Reutter, P., Su, H., Trentmann, J., Simmel, M., Rose, D., Gunthe, S. S., Wernli, H., Andreae, M. O., and Pöschl, U. (2009). Aerosoland updraft-limited regimes of cloud droplet formation: influence of particle number, size and hygroscopicity on the activation of cloud condensation nuclei (CCN). *Atmos. Chem. Phys.*, 9, 7067–7080.

Riipinen, I., Yli-Juuti, T., Pierce, J. R., Petäjä, T., Worsnop, D. R., Kulmala, M., and Donahue, N. M. (2012). The contribution of organics to atmospheric nanoparticle growth. Nature Geoscience, 5:453-458.

Romakkaniemi, S., Kokkola, H., and Laaksonen, A. (2005b). Soluble trace gas effect on cloud condensation nuclei activation: Influence of initial equilibration on cloud model results. *J. Geophys. Res.*, 110: D15202.

Romakkaniemi, S., McFiggans, G., Bower, K. N., Brown, P., Coe, H., and Choularton, T. W. (2009). A comparison between trajectory ensemble and adiabatic parcel modeled cloud properties and evaluation against airborne measurements. *J. Geophys. Res.*, 114, D06214.

Rosenfeld, D., Sherwood, S., Wood, R., and Donner, L. (2014). Climate effects of aerosol-cloud interactions. *Science*, 343(6169), 379–380.

Russell, A.G., Winner, D.A., Harley, R.A., McCue, K.F., and Cass, G.R. (1993). Cass Mathematical modeling and control of the dry deposition flux of nitrogen-containing air pollutants. *Envir. Sci. Technol.*, 27, 2772–2782.

Salter, S. Sortino, G. and Latham, J. (2008). Sea-going hardware for the cloud albedo method of reversing global warming. Philosophical Transactions of the Royal Society A: Mathematical. *Physical and Engineering Sciences.*, 366, 3989–4006.

Sand, M., Berntsen, T. K., Seland, Ø., and Kristjansson, J. E. (2013). Arctic surface temperature change to emissions of black carbon within Arctic or midlatitudes. *J. Geophys. Res.*, 118, 7788–7798.

Schobesberger, S., Junninen, H., Bianchi, F., Lönn, G., Ehn, M., Lehtipalo, K., Dommen, J., Ehrhart, S., Ortega, I. K., Franchin, A., Nieminen, T., Riccobono, F., Hutterlie, M., Duplissy, J., Almeida, J., Amorim, A., Breitenlechner, M., Downard, A. J., Dunne, E. M., Flagan, R. C., Kajos, M., Keskinen, H., Kirkby, J., Kupc, A., Kürten, A., Kurt_en, T., Laaksonen, A., Mathot, S., Onnela, A., Praplan, A. P., Rondo, L., Santos, F. D., Schallart, S., Schnitzhofer, R., Sipilä, M., Tom_ef, A., Tsagkogeorgas, G., Vehkamäki, H., Wimmer, D., Baltensperger, U., Carslaw, K. S., Curtius, J., Hansel, A., Petäjä, T., Kulmala, M., Donahue, N. M., and Worsnop, D. R. (2013). Molecular understanding of atmospheric particle formation from sulfuric acid and large oxidized organic molecules Proc. Nat. Acad. Sci., 110(43):17223-17228.

Seifert, A. and Beheng, K. D. (2006). A two-moment cloud microphysics parameterization for mixed-phase clouds. Part 2: Maritime vs. continental deep convective storms, *Meteor. Atmos. Phys.*, 92, 45–66.

Seifert A, Heus T, Pincus R, and Stevens B. (2015). Large-eddy simulation of the transient and near-equilibrium behavior of precipitating shallow convection. *J Adv Model Earth Syst.* 7, 1918–1937.

Seinfeld, J. H., and Pandis, S. N. (2006). Atmospheric Chemistry and Physics: From air pollution to climate change. Wiley: NY.

Seinfeld, J.H., Bretherton, C., Carslaw, K.S., Coe, H., DeMott, P.J., Dunlea, E.J., Feingold, G., Ghan, S., Guenther, A.B., Kahn, R., Kraucunas, I., Kreidenweis, S.M., Molina, M.J., Nenes, A., Penner, J.E., Prather, K.A., Ramanathan, V., Ramaswamy, V., Rasch, P.J., Ravishankara, A.R., Rosenfeld, D., Stephens, G., Wood, R. (2016). Improving our fundamental understanding of the role of aerosol-cloud interactions in the climate system. PNAS 113 (21), 5781–5790.

Shepherd, J., (2009). Geoengineering the climate: Science, governance and uncertainty. *Report of the Royal Society*, London.

Siebesma, A.P., Brown, C.S.B.A., Chlond, A., Cuxart, J., Duynkerke, P., Jiang, H., Khairoutdinov, M., Lewellen, D., Moeng, C.-H., Sanchez, E., Stevens, B., and Steven, D.E.

(2003). A large eddy simulation intercomparison study of shallow cumulus convection. *J. Atmos. Sci.,* 60, 1201–1219.

Stevens, B., Lenschow, D.H., Faloona, I., Moeng, C.-H., Lilly, D.K., Blomquist, B., Vali, G., Campos, T., Gerber, H., Haimov, S., Morley, B., and Thornton, D. (2003). On entrainment in nocturnal marine stratocumulus. *Q. J. R.Meteor. Soc.,* 129:3469–92.

Stevens, B., Moeng, C.-H., Ackerman, A.S., Bretherton, C.S., Chlond, A., de Roode, S., Edwards, J., Golaz, J.-C., Jiang, H., Khairoutdinov, M., Kirkpatrick, M.P., Lewellen, D.C., Lock, A., Müller, F., Stevens, D.E., Whelan, E., and Zhu, P. (2005). Evaluation of large-eddy simulations via observations of nocturnal marine stratocumulus. *Mon. Weather Rev.,* 133, 1443–1462.

Stevens, B., and Seifert, A. (2008). Understanding macrophysical outcomes of microphysical choices in simulations of shallow cumulus convection. *J. Meteorol. Soc. Jpn.,* 86, 143–162.

Stier, P., Seinfeld, J. H. Kinne, S. and Boucher, O. (2007). Aerosol absorption and radiative forcing. *Atmos. Chem. Phys.,* 7, 5237–5261.

Stocker T. F., Qin D., Plattner G. K., Tignor M., Allen S. K., Boschung J., Nauels, A., Xia, Y., Bex, V. and Midgley, P. M. (2013). IPCC, 2013: Climate Change 2013: The Physical Science Basis. Contribution of Working Group I to the Fifth Assessment Report of the Intergovernmental Panel on Climate Change. Cambridge: Cambridge University Press.

Stolaki, S., Pytharoulis, I., and Keracostas, T. (2015). A study of fog characteristics using acoupled WRF-Cobel model over Thessaloniki airport, Greece. *Pure Appl. Geophys.*, 169, 961–981.

Stuart, G. S., Stevens, R. G., Partanen, A.-I., Jenkins, A. K. L., Korhonen, H., Forster, P. M., Spracklen, D. V., and Pierce, J. R. (2013). Reduced efficacy of marine cloud brightening geoengineering due to in-plume aerosol coagulation: parameterization and global implications. *Atmos. Chem. Phys.,* 13, 10385–10396.

Stull, R. B. (1988). An Introduction to Boundary Layer Meteorology.

Tao, W.-K., Chern, J.-D., Atlas, R., Randall, D., Khairoutdinov, M., Li, J.-L., Waliser, D.E., Hou, A., Lin, X., Peters-Lidard, C., Lau, W., Jian, J., Simpson, J. (2009). A Multiscale

Modeling System: Developments, applications, and critical issues. *Bull. Am. Meteor. Soc.*, 90, 515–534.

Tomita, H., Miura, H. Iga, S. Nasuno, T. and Satoh, M. (2005). A global cloud-resolving simulation: Preliminary results from an aqua planet experiment. *Geophys. Res. Lett.*, 32, 08805.

Tsigaridis, K., Daskalakis, N., Kanakidou, M., Adams, P. J., Artaxo, P., Bahadur, R., Balkanski, Y., Bauer, S. E., Bellouin, N., Benedetti, A., Bergman, T., Berntsen, T. K., Beukes, J. P., Bian, H., Carslaw, K. S., Chin, M., Curci, G., Diehl, T., Easter, R. C., Ghan, S. J., Gong, S. L., Hodzic, A., Hoyle, C. R., Iversen, T., Jathar, S., Jimenez, J. L., Kaiser, J. W., Kirkevåg, A., Koch, D., Kokkola, H., Lee, Y. H., Lin, G., Liu, X., Luo, G., Ma, X., Mann, G. W., Mihalopoulos, N., Morcrette, J.-J., Müller, J.-F., Myhre, G., Myriokefalitakis, S., Ng, S., O'Donnell, D., Penner, J. E., Pozzoli, L., Pringle, K. J., Russell, L. M., Schulz, M., Sciare, J., Seland, Ø., Shindell, D. T., Sillman, S., Skeie, R. B., Spracklen, D., Stavrakou, T., Steenrod, S. D., Takemura, T., Tiitta, P., Tilmes, S., Tost, H., van Noije, T., van Zyl, P. G., von Salzen, K., Yu, F., Wang, Z., Wang, Z., Zaveri, R. A., Zhang, H., Zhang, K., Zhang, Q., and Zhang, X. (2014). The AeroCom evaluation and intercomparison of organic aerosol in global models, Atmos. Chem. Phys., 14, 10845-10895.

Twomey, S.A. (1977). The influence of pollution on the shortwave albedo of clouds, *J. Atmos. Sci.*, 34, 1149–1152.

van Zanten, M.C., Stevens, B., Nuijens, L., Siebesma, A.P., Ackerman, A.S., Burnet, F., Cheng, A., Couvreux, F., Jiang, H., Khairoutdinov, M., Kogan, Y., Lewellen, D.C., Mechem, D., Nakamura, K., Noda, A., Shipway, B.J., Slawinska, J., Wang, S., and Wyszogrodzki, A. (2011). Controls on precipitation and cloudiness in simulations of trade-wind cumulus as observed during RICO. *J. Adv. Model. Earth Syst.*, 3: M06001.

Vaughan, N., and Lenton, T. (2011). A review of climate geoengineering proposals. *Climatic Change*., 109 (3–4), 791–825.

Vautard, R., Yiou, P., and Van Oldenborgh, G.J. (2009). Decline of fog, mist and haze in Europe over the past 30 years. *Nat. Geosci.*, 2: 115e119.

Väänänen, R., Kyrö, E.-M., Nieminen, T., Kivekäs, N., Junninen, H., Virkkula, A., Dal Maso, M., Lihavainen, H., Viisanen, Y., Svenningsson, B., Holst, T., Arneth, A., Aalto, P. P., Kulmala, M., and Kerminen, V.-M. (2013). Analysis of particle size distribution changes

between three measurement sites in northern Scandinavia. *Atmos. Chem. Phys.*, 13, 11887–11903.

Väisänen, O., Ruuskanen, A., Ylisirniö, A., Miettinen, P., Portin, H., Hao, L., Leskinen, A., Komppula, M., Romakkaniemi, S., Lehtinen, K.E.J., and Virtanen, A. (2016). In-cloud measurements highlight the role of aerosol hygroscopicity in cloud droplet formation. *Atmos. Chem. Phys.*, 16, 10385-10398.

Walcek, C.J., and Chang, J.S. (1987). A theoretical estimate of pollutant deposition to individual land types during a regional-scale acid deposition episode. *Atmos. Environ.*, 21, 1107–1113, 1987.

Wang, H., Rasch, P.J., and Feingold, G. (2011). Manipulating marine stratocumulus cloud amount and albedo: a process-modelling study of aerosol-cloud-precipitation interactions in response to injection of cloud condensation nuclei. *Atmos. Chem. Phys.*, 11, 4237–4249.

Williams, J., de Reus, M., Krejci, R., Fischer, H., and Strm, J. (2002). Application of the variability-size relationship to atmospheric aerosol studies: estimating aerosol lifetimes and ages. *Atmos. Chem. Phys.*, 2, 133–145.

Wood, R. (2012). Review: Stratocumulus clouds. *Mon. Wea. Rev.*, 140: 2373–2423.

Wu, Z. J., Hu, M., Lin, P., Liu, S., Wehner, B., and Wiedensohler, A. (2008). Particle number size distribution in the urban atmosphere of Beijing. *China, Atmos. Environ.*, 42, 7967–7980.

Zhang, L., Gong, S.-L., Padro, J., and Barrie, L. (2001). A Size-segregated Particle Dry Deposition Scheme for an Atmospheric Aerosol Module. *Atmos. Environ.*, 35(3), 549–560.

Zhang, X., Musson-Genon, L., Dupont, E., Milliez, M., Carissimo, B. (2014). On the Influence of a Simple Microphysics Parametrization on Radiation Fog Modelling: A case study during ParisFog. *Boundary-Layer Meteorol.* 151,293–315.